



University of Stuttgart
Institute of Interfacial Process Engineering
and Plasma Technology

Annual Report 2020–2022



Editorial notes

Institute of Interfacial Process Engineering and Plasma Technology IGVP
University of Stuttgart
Pfaffenwaldring 31, 70569 Stuttgart, Germany
www.igvp.uni-stuttgart.de
institut@igvp.uni-stuttgart.de

Director

Prof. Dr. habil. Günter Tovar (acting)

Phone +49 711 685-62304

Fax +49 711 685-63102

Layout

Dipl.-Des. Thaya Schroeder M. Sc.

Annual Report 2020–22

**Institute of Interfacial Process Engineering
and Plasma Technology**
University of Stuttgart

Preface



The past three years have clearly shown us how essential high-performance research is. Strong in the fundamentals, ready for application and committed to goal-oriented collaboration. This is precisely how the course for pandemic control was set in record time on the basis of high-performance research. These attributes described above also characterize the way we see ourselves and our work at the Institute of Interfacial Process Engineering and Plasma Technology (IGVP) at the University of Stuttgart. This Three-Year Report 2020–22 provides a cross-section of our research, we are dedicated to application-oriented and highly networked basic research.

The sustainability of future technologies is a clear goal for us at IGVP and is a constant concern for us. In doing so, we are guided by the plausible mission statement that the United Nations (UN) already established for itself at the end of 2015. Coincidentally, this happened at the same time that I myself was entrusted with the acting leadership of the IGVP. Since then, we at the IGVP have been repeatedly inspired and motivated by the seventeen Sustainable Development Goals (SDGs) and are gradually and ever more consistently aligning our research with these guiding principles into the future. It therefore seems only logical to structure this triennial report in terms of the SDGs, and to organize our work within this framework.

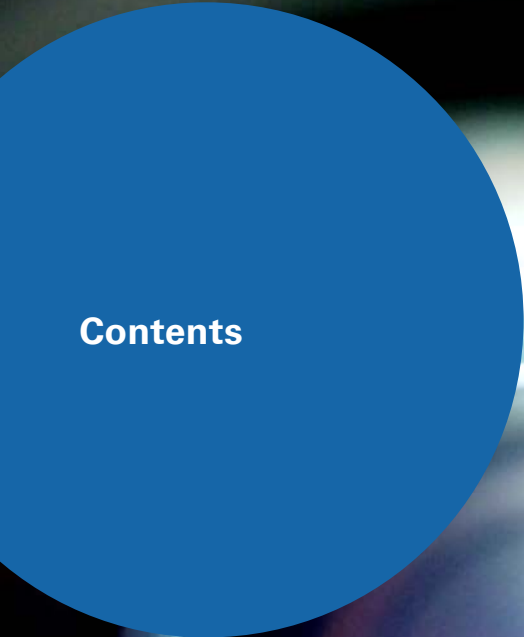
Our research is essentially aimed at value creation. A main line of development ranges from the generation of usable basic chemicals by means of plasma-chemical innovations, for example by recycling CO₂, to the biotechnological production of life molecules with microalgae or insect larvae, to the biofabrication of complex functional matrices for medical technology or the construction technology of the future. The functionalization of technical interfaces as well as software- and hardware-oriented component development for the energy generation of the future also remain in our focus.

At the IGVP, we are well interconnected through excellent national and international partnerships. We are particularly pleased about the very cooperative collaboration with the Fraunhofer Institute for Interfacial Engineering and Biotechnology (IGB) in Stuttgart and the Max Planck Institute for Plasma Physics (IPP) in Garching and Greifswald. We are also proud to be a founding member of three trend-setting alliances at the University of Stuttgart and to be intensively involved in promoting the research location: In the Stuttgart Research Initiative (SRI) CHEMAmpere, we want to enable sustainable CO₂-neutral production of chemicals; in the SRI Valorization of Bioresources (SRI ValBio), we are dedicated to sustainable management through the establishment of material cycles with intensive use of renewable biological resources. The Stuttgart Partnership Initiative Mass Personalization (SPI-MP) focuses on excellent basic research into manufacturing and biomaterial technologies for personalized biomedical systems.

At the IGVP, we conduct independent and highly networked research in a variety of constellations, some of which are presented in this triennial report. We hope you enjoy and find fascinating insights as you explore the IGVP's research.



Prof. Dr. habil. Günter Tovar (acting director)



Contents



10 IGVP Profile

12 Members of the Institute

16 RESEARCH RESULTS

18 SDG 3: GOOD HEALTH AND WELL-BEING

- 20 Particle-based formulations for the intranasal transmucosal delivery of biopharmaceuticals
- 21 Integration of isothiuronium groups for biofunctionalization of hydrogels
- 22 Generation and characterization of azide-modified extracellular matrix as click-chemically crosslinkable biomaterial
- 24 Methacrylated biomaterials for 3D bioprinting of personalized cartilage and tendon implants
- 25 Physical and chemical cross-linking of gelatin-methacryloyl as scaffold for articular cartilage equivalents
- 27 Development of a bio-based particulate drug delivery system for nose-to-brain transport of mAbs
- 29 Bio2Brain: Bio-based hydrogels as drug delivery systems for the intranasal transmucosal delivery of biopharmaceuticals

30 SDG 6: CLEAN WATER AND SANITATION

- 32 Energetic and economic viability of active atmospheric water generation technologies
- 33 Hydrogels as functional coatings for sensor applications

34 SDG 7: AFFORDABLE AND CLEAN ENERGY

- 36 Numerical investigation of hydrogen plasma from the Duo-Plasmaline in a magnetic field
- 37 Experimental investigation of hydrogen plasma from the Duo-Plasmaline in a magnetic field
- 38 Design of a focusing horn antenna for a correlation ECE system for W7-X
- 39 Generation of a homogeneous microwave field for an ECEI detector array
- 40 Development of diffraction gratings for advanced ECRH scenarios
- 41 Simulation of the microwave optics for the first plasma in ITER
- 42 Calculations for the EBW-launcher for MAST Upgrade
- 43 Design of a hole array for use as a dual frequency power monitor for high power transmission lines
- 44 PROFUSION code development

- 45 Microwave absorbing layer materials for fusion reactors
- 46 Fullwave Doppler reflectometry simulations for ASDEX Upgrade
- 48 Optimisation of a broadband antenna for plasma positioning reflectometry
- 49 Fullwave 3D simulations of an ICRF antenna interferometer
- 50 Fullwave 3D simulations of diffraction losses in a 170 GHz miterbend
- 51 Comb reflectometer backend for fusion plasmas
- 52 Plasma dynamical processes in generation and confinement
- 53 Numerical feasibility study of electron Bernstein wave heating in LTX- β
- 54 Simulation of the O-SX-B mode conversion process in the TJ-K stellarator
- 55 Plasma electrons' acceleration up to energies of 100 keV
- 56 Influence of plasma density fluctuations on wave coupling scenarios
- 57 FDTD full-wave simulations and interferometry measurements for microwave-plasma interactions
- 58 Tilt angle analysis of turbulent structures with the ellipsoidal model
- 59 Enhancement of energy transfer to zonal flows by stationary shear flows
- 60 Interplay of turbulent density and momentum transport in TJ-K plasmas
- 61 Causality analysis of the drift-wave – zonal flow system at the stellarator TJ-K
- 62 Collisionality dependence of spectral power distribution
- 63 Turbulence classification using artificial neural networks
- 64 Investigation into the spatial distribution of intermittency at the stellarator TJ-K
- 65 Non-locality of particle transport in the stellarator TJ-K
- 66 Turbulence transport across magnetic islands

68 SDG 9: INDUSTRY, INNOVATION AND INFRASTRUCTURE

- 70 Emission spectroscopic and high-speed camera measurements at water vapor arc plasma
- 72 Optical emission spectroscopy of a CO₂/H₂ microwave plasma
- 73 NO_x production in an atmospheric plasma torch
- 74 Cross-linking and permeability of polyvinyl alcohol coatings for the humidification of fuel cells
- 76 Organic waste as a renewable resource – conversion of the fat and protein content of *Hermetia illucens*

78 SDG 11: SUSTAINABLE CITIES AND COMMUNITIES

- 80 Immobilization of microalgae in hydrogels
- 81 Application of adhesion-promoting layers via plasma polymerisation on glass fibers

82 SDG 12: RESPONSIBLE CONSUMPTION AND PRODUCTION

- 84** Synthesis and investigation of hybrid structural composites
- 85** Tribology system for cold sheet metal forming based on volatile lubricants
- 86** Design of a nozzle geometry for the formation of an atmospheric pressure microwave plasma flow

88 SDG 13: CLIMATE ACTION

- 90** Numerical investigation of a microwave plasma torch for CO₂ decomposition
- 91** Enhancing CO₂ conversion through an optimization in the gas management
- 92** Oxygen separation with ceramic hollow fibers in a CO₂ plasma
- 94** High-temperature oxygen separation performance of dual-phase ceramic material
- 95** Ceramic membrane material screening for high-temperature oxygen permeation
- 96** CO₂ conversion and energy efficiency of a microwave plasma torch
- 97** Photomodulation of the mechanical properties of a chitosan-based composite material

98 SDG 14: LIFE BELOW WATER

- 100** Optimization of a DBD plasma for the deposition of protective films in heat exchangers
- 101** sPlash – Plasma-coated hydrophobic textiles for cleaning oil spillage in inland waterways

102 SDG 15: LIFE ON LAND

- 104** Production of the beta-glucan chrysolaminarin from microalgae in closed photobioreactor systems
- 105** Integrated process design and optimization of cellobiose lipids fermentation and purification
- 106** Mineral composites as DBD layers in a plasma-adsorber-scrubber-system for waste air treatment

The direct link to our peer-reviewed publications goes

www.igvp.uni-stuttgart.de/forschung/publikationen

Profile of the Institute

The Institute of Interfacial Process Engineering and Plasma Technology IGVP at the University of Stuttgart is dedicated to mostly interdisciplinary and multidisciplinary research and teaching in the field of Materials Science, Life Sciences, Process Engineering and Plasma Sciences and is inspired by the global sustainability goals, to which the United Nations, the Federal Government of Germany and the State Government of Baden-Württemberg are also committed.



Key Figures

The research budget amounted to 2.3 million euros in 2020, 2.2 million euros in 2021 and 2.3 million euros again in 2022. At the end of 2022, 64 scientific, technical and administrative members of the IGVP team were active, including 39 young scientists working on their dissertations. We also hosted 52 students, 42 researching for their Master's thesis and 10 for their Bachelor's thesis.

Organization and Facilities

The IGVP is part of the Faculty 4: Energy-, Process- and Bio-Engineering of the University of Stuttgart. State-of-the-art labs, technical plants and workshops are available at the IGVP for research in natural sciences and interdisciplinary engineering. They are located at the three IGVP facilities in Pfaffenwaldring 31, Allmandring 5b at the University Campus and within the Fraunhofer Institute for Interfacial Engineering and Biotechnology IGB in Nobelstrasse 12.

Research

We explore the use, design, modeling and functionalization of interfaces, surfaces and interfacial processes. Our focus aims to further develop technologies in the sense of the Sustainable Development Goals or to make them possible in the first place (proof-of-concept). In particular, we use bio- and nanomaterials as well as bio- and plasma-technical processes and very often work together with research

partners. The IGVP is founding member of the Stuttgart Partnership Initiative Mass Personalization (SPI-MP), the Stuttgart Research Center Systems Biology (SRCSB), and the Stuttgart Research Initiatives CHEMampere and Valorization of Bioresources (ValBio).

Collaboration

Close cooperation of the IGVP with Fraunhofer IGB enables a dynamic collaboration between researchers and lecturers of both institutions and furthermore allows to pursue projects from basic research to application. This approach is reflected in the variety of funding received by the IGVP, including funds from the Land of Baden-Württemberg, from Federal Ministries (e.g. BMBF), from the German Research Foundation (DFG), from the German Federal Foundation for the Environment (DBU), from the EU and from various foundations as well as from industry.

Since many years, the Max Planck Institute for Plasma Physics (IPP), located in Garching and Greifswald, is another key partner of the IGVP and is enabling us to maintain a leading role in plasma technology. You can find more research alliances on our website.

Teaching

The IGVP is highly active in teaching both within master and bachelor study programs at the University of Stuttgart, especially in the programs on Process Engineering, Medical Technology, Technical Biology, Energy Technology, Renewable Energy Engineering, Environmental Engineering, WASTE and Environmental Engineering.

Thematic Focus

- Interfacial process engineering
- Nanomaterials and nanotechnology
- Biomaterials and infection biology
- Renewable raw materials, industrial biotechnology and bioenergy
- Plasma technology and plasma physics
- Microwave technology for plasmas and process engineering

Contact

Institute of Interfacial Process Engineering and Plasma Technology IGVP
University of Stuttgart
Pfaffenwaldring 31, 70569 Stuttgart, Germany
Fax +49 711 685-63102 • www.igvp.uni-stuttgart.de

Prof. Dr. habil. Günter E. M. Tovar
Director (acting)
Phone +49 711 685-62304
guenter.tovar@igvp.uni-stuttgart.de

Dr.-Ing. Matthias Walker
Head of Administration
Phone +49 711 685-62300
matthias.walker@igvp.uni-stuttgart.de

Members of the Institute 2020–2022

Director

Prof. Dr. Günter Tovar (acting)

Professors

Prof. Dr. Susanne Bailer

Prof. Dr. Achim Lunk (retired)

Prof. Dr. Christian Oehr (retired)

Prof. Dr. Steffen Rupp

Prof. Dr. Uwe Schumacher (retired)

Assistance

Ingeborg Wagner

Administration

Dr.-Ing. Matthias Walker (Head)

Ruth Edelmann-Amrhein (until March 2022)

Irina Löffler (since June 2021)

Sibel Sevik

Personnel

Eva Mühlbauer M. A. (until May 2020)

Bianca Zeindlmeier (until May 2020)

IT

Sven Marvin Oesterle (since October 2020)

Dr.-Ing. Burkhard Plaum

Stuttgart Research Initiative Mass Personalization

Janina Ulmer (since January 2022)

Mechanical Workshop and Engineering Design

Felix Rempel (Head)

Muhammed Acar (until May 2022)

Wolfgang Baur (until May 2022)

Athanasios Dallas (Apprentice since September 2022)

Emma Echeverria Ortiz (since July 2022)

Redur Khalaf (since June 2022)

Manfred Krämer (until March 2021)

Emre Okuyan (Apprentice until August 2021)

Emily Seeger (Apprentice since September 2022)

Levin Senela (Apprentice)
Sven Sorichta

Electrical Workshop and Electronics

Holger Röhlinger (Head)
Murat Basar (Apprentice)
Christian Dantas-Gamerding (Apprentice since September 2022)
Tanju Haspel (Apprentice until December 2021)
Jonas Klöpfer (Apprentice)
Jael Linda Scherr (Apprentice)
Thomas Selzer (Apprentice since September 2022)
David Zander (since December 2020)

LIFE SCIENCES

Principal Investigators:

Prof. Dr. Susanne Bailer (Head)
Prof. Dr. Steffen Rupp
Dr. Anke Burger-Kentischer
Dr. Gabriele Vacun (until August 2021)

Research Staff:

Lilija Ignatjew (until November 2021)
Débora Marques (until January 2020)
Helena Merk (until August 2020)
Eileen Sauer

MATERIALS SCIENCE

Principal Investigators:

Dr. Alexander Southan (Head until December 2022)

Research Staff:

Vanessa Albernaz
Beatrice Di Lelio (since October 2021)
Oliver Gorke (until January 2021)
Jana Grübel (until December 2021)
Silke Keller (until January 2020)
Andre Michele (until September 2021)
Pinar Koca (since August 2021)

Julius Potyka (since June 2022)
Lisa Rebers (until July 2020)
Paul Reichle
Julia Rotenberger (until July 2020)
Lena Marie Spindler (until January 2022)
Erik Taylor (since October 2021)
Anastasia Tsianaka

BIOINSPIRED MATERIAL CHEMISTRY

Principal Investigators:

Dr. Linus Stegbauer (Head)
Dr. Amrita Rath (until December 2021)

Research Staff:

Tugce Demiral (since October 2021)
Nina Oehlsen (since October 2021)
Nils von Seggern (since February 2020)

PROCESS ENGINEERING

Principal Investigators:

Dr.-Ing. Matthias Stier (Head until August 2020)
Dr.-Ing. Susanne Zibek (Head since September 2020)
Dr. Ana Lucia Vásquez-Caicedo Le Roux (until June 2020)

Research Staff:

Fredy-Wsbaldo Baron Nunez
Alexander Beck
Vroni Czotscher (since March 2022)
Ilka Derwenskus (until February 2021)
Muhand Fadlalla Elamin (since February 2022)
Konstantin Frick
Kuan-Po Liao (since March 2022)
Ilka Mühlemeier (until March 2022)
Amira Oraby
Ricardo Reyes Alva (since March 2022)
Christian Schmidle (since April 2022)
Dr. Nicole Werner (until January 2021)
Yen-Cheng Yeh

PLASMA TECHNOLOGY

Principal Investigators:

Dr.-Ing. Matthias Walker (Head)

Dr. Andreas Schulz

Research Staff:

Marc Bresser (since April 2022)

Irina Kistner

Dr. Stefan Merli

Heinz Petto

Steffen Pauly (until April 2022)

Dr. Mariagrazia Troia

Katharina-Sophia Wiegers

PLASMA DYNAMICS AND DIAGNOSTICS

Principal Investigators:

Dr. Mirko Ramisch (Head)

Dr. Eberhard Holzhauer (Retired)

Dr. Alf Köhn-Seemann

Research Staff:

Nicolas Dumérat (since November 2020)

Bernhard Roth

Ralph Sarkis (since June 2022)

Dr. Bernhard Schmid (until May 2021)

Dr. Til Ullmann (since December 2020)

Christos Vagkidis (since February 2022)

MICROWAVE TECHNOLOGY

Principal Investigators:

Dr. Carsten Lechte (Head)

Dr.-Ing. Walter Kasperek (Retired)

Dr.-Ing. Burkhard Plaum

Research Staff:

Andreas Hentrich (since January 2021)

Achim Zeitler



Research results

In the following we present a number of research results. They are sorted according to their main reference-SDG. Further research topics can be found on our homepage.

The direct link to our peer-reviewed publications goes www.igvp.uni-stuttgart.de/forschung/publikationen

3 GOOD HEALTH AND WELL-BEING



Particle-based formulations for the intranasal transmucosal delivery of biopharmaceuticals

Beatrice Di Lelio, Carmen Gruber-Traub, Günter Tovar



Biopharmaceuticals like monoclonal antibodies are an attractive new strategy to face many neurological disorders with unmet medical needs, such as Multiple sclerosis. Unfortunately, antibodies are mainly used as injectable drugs and often face a low bioavailability in the central nervous system due to the presence of the blood-brain-barrier. Nose-to-brain drug delivery is an attractive alternative for the administration of drugs directly to the brain.

The project aims to develop a bio-based particle system for the encapsulation and the transmucosal delivery of biopharmaceutical through the olfactory mucosa, ensuring a controlled release through the mucosa and a better stability of the encapsulated biopharmaceutical. To achieve this goal, biopolymers such as chitosan will be chemically modified with thiol moieties, so to improve their mucoadhesive properties and introduce new functional groups available for crosslinking. The resulting material will then be used to produce particles through spray drying, a one step, scalable method that ensures a gentle encapsulation of heat sensible active pharmaceutical ingredients.

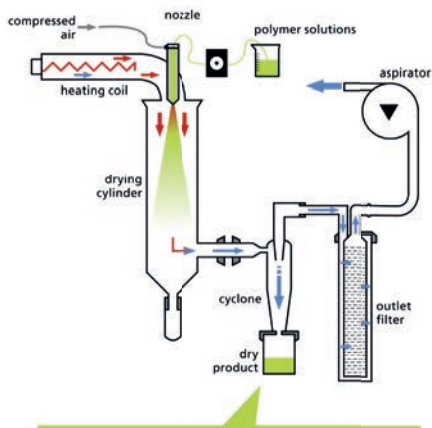


Fig. 1: Schematic representation of the spray drying process.

Collaboration: Carmen Gruber-Traub and Michaela Müller, Fraunhofer Institute for Interfacial Engineering and Biotechnology IGB, Stuttgart

Funding: This project has received funding from the European Union's Horizon 2020 research and innovation programme under the Marie Skłodowska-Curie grant agreement No 956977

Integration of isothiuronium groups for biofunctionalization of hydrogels

Jana Grübel, Anastasia Tsianaka, Alexander Southan, Günter Tovar

Hydrogels based on poly(ethylene glycol) (PEG) are widely applied in tissue engineering, drug delivery and for biosensors. With their bioinert surface they inhibit protein adsorption and cell adhesion but the properties of the hydrogels can be altered with various methods.

To functionalize PEG-based hydrogels we integrate isothiuronium groups in a one step process. These groups are known to have anti-tumor activity and antimicrobial effects. Since they can also be reduced to thiols, they enable to bind other molecules to the hydrogels. The successful functionalization of the hydrogels was determined by analytical methods like the measurement of the contact angle, the zeta potential, and the adsorption of the drug diclofenac. The reduction of the isothiuronium groups to thiols was demonstrated by binding a fluorescent dye or enzyme to the

hydrogels. Furthermore the functional groups were used to bind spatial distributed gelatin-based coatings on the hydrogel surfaces. With different bioink compositions the hydrogels can serve as a biosensor platform for various substrates.

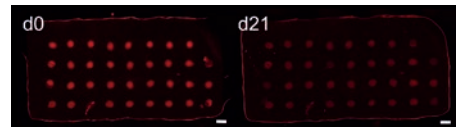


Fig. 2: Fluorescence staining of printed gelatin spots on PEG-based hydrogels. Spots were stained with fluorescent nanoparticles and fluorescence intensity was evaluated over 21 days, scale bar 1 mm.

Publication: Grübel, J., Albernaz, V. L., [...], Southan, A. Multifunctional hydrogels with accessible isothiuronium groups can be prepared by radical cross-linking, submitted in *Journal of Materials Science*

Collaboration: Fraunhofer Institute for Interfacial Engineering and Biotechnology IGB, Stuttgart

Funding: PhD scholarship of the Evonik Foundation

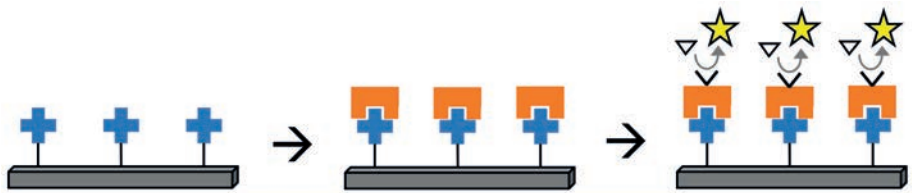


Fig. 1: Schematic visualization of functionalized PEG-based hydrogels. Isothiuronium groups are introduced by copolymerization of a monomer with the macromonomers. With the functional groups on the hydrogel surface a bioactive coating can be bound which can serve as a biosensing platform.



Generation and characterization of azide-modified extracellular matrix as click-chemically crosslinkable biomaterial

Silke Keller, Alexander Southan, Günter Tovar

Biomaterials are materials that interact with biological systems in order to treat, augment or replace any tissue, organ, or function of the body. These materials have to meet certain mechanical requirements and have to be compatible with the human body. Depending on the envisaged application, it can be desirable that they affect the biological activities and responses of the cells in the immediate vicinity.

In a natural tissue the extracellular matrix (ECM) resembles the natural microenvironment of cells. Due to its high biological activity, the isolated ECM is a promising biomaterial for the use in tissue engineering and regenerative medicine. However, the use of ECM is limited, e. g. due to the lack of

specific functional groups which are often required for their use as coatings or scaffolds.

Thus, the approach of this work was to develop an azide-functional ECM which resembles the natural, tissue-specific ECM composition of the body and which can furthermore be addressed in a bio-compatible chemical reaction (azide-alkyne cycloaddition). Therefore, we incorporated azide groups as chemical handles into the ECM glycoconjugates by Metabolic Glyco-Engineering. The resulting so called *clickECM* can e. g. be selectively conjugated in a bioorthogonal azide-alkyne-cycloaddition with different with alkyne-functional drugs or biomolecules or it can be immobilized on alkyne-functionalized surfaces to

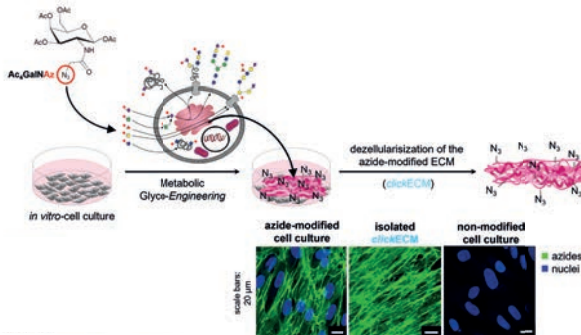


Fig. 1: Top scheme: Metabolic Glyco-Engineering to generate an azide-modified extracellular matrix ("*clickECM*").

Figure lower right-hand corner: Detection of the fluorophore-conjugated azides within the *clickECM* via Laser-Scanning-Microscopy.

form stable surface coatings to enhance cell adhesion.

Applied as a surface coating, it was possible to produce homogeneous and bioactive coatings which were stable against fluid mechanical abrasion. By conjugating the *click*ECM azides in these layers with alkyne-coupled biotin molecules, the layers could be successfully biotinylated to set up a universal bioconjugation platform based on the versatile biotin-streptavidin interaction. In this way, it was possible to equip the *click*ECM layers with additional functions not naturally occurring in the ECM, such as horseradish peroxidase.

Publications: Keller, S., Liedek, A., Shendi, D., Bach, M., Tovar, G.E.M., Kluger, P. J., Southan, A. (2020) Eclectic Characterisation of Chemically Modified Cell-Derived Matrices Obtained by Metabolic Glycoengineering and Re-Assessment of Commonly Used Methods, *RSC Advances*, 10(58) 35273-35286. <https://doi.org/10.1039/D0RA06819E>
 Keller, S., Wörgötter, K., Liedek, A., Kluger, P. J., Bach, M., Tovar, G. E. M., Southan, A. (2020) Azide-functional extracellular matrix coatings as bioactive platform for bioconjugation, *ACS Applied Materials & Interfaces*, 12(24), 26868–26879. <https://doi.org/10.1021/acsami.0c04579>
 Keller, S., Bakker, T., Kimmel, B., Rebers, L., Götz, T., Tovar, G. E. M., Kluger, P. J., Southan, A. (2021) Azido-functionalized gelatin via direct conversion of lysine amino groups by diazo transfer as a building block for biofunctional hydrogels, *Journal of Biomedical Materials*

Research Part A, 109(1), 77–91. <https://doi.org/10.1002/jbm.a.37008>
 Ruff*, S. M., Keller*, S., Wieland, D. E., Wittmann, V., Tovar, G. E. M., Bach, M., Kluger, P. J. (2017) *click*ECM: Development of a cell-derived extracellular matrix with azide functionalities, *Acta Biomaterialia*, 52, 159–170. <https://doi.org/10.1016/j.actbio.2016.12.022> (*shared first co-authorship)
 Shendi, D., Marzi, J., Linthicum, W., Rickards, A. J., Dolivo, D. M., Keller, S., Kauss, M. A., Wen, Q., McDevitt, T. C., Dominko, T., Schenke-Layland, K., Rolle, M. W. (2019) Hyaluronic acid as a macromolecular crowding agent for production of cell-derived matrices, *Acta Biomaterialia*, 100, 292–305. <https://doi.org/10.1016/j.actbio.2019.09.042>
 Nellinger, S., Keller, S., Southan, A., Wittmann, V., Volz, A.-C., Kluger, P. (2019) Generation of an azide-modified extracellular matrix by adipose-derived stem cells using metabolic glycoengineering, *Current Directions in Biomedical Engineering*, 5, 393–395. <https://doi.org/10.1515/cdbme-2019-0099>

Collaboration: Fraunhofer Institute for Interfacial Engineering and Biotechnology IGB, Stuttgart; Reutlingen University, School of Applied Chemistry, Reutlingen; University of Konstanz, Department of Chemistry and Konstanz Research School Chemical Biology, Konstanz; University of Hohenheim, Module 3: Analytical Chemistry Unit, Stuttgart

Funding: PhD scholarship of the Peter und Traudl Engelhorn Stiftung; Baden-Württemberg Bioeconomy Research Program of the Baden-Württemberg Stiftung and the Ministry of Science, Research and the Arts of the State of Baden-Württemberg (“Glykobiologie/ Glykobiotechnologie”, reference no. 33-7533-7-11.9/7/2; Vector Stiftung (grant number: P2015-0052); Baden-Württemberg Stiftung (“Glycobiology/Glycomics”, grant no.: P-BWS-Glyko/09); Fraunhofer Internal Programs Discover (grant number: Discover 828 355)

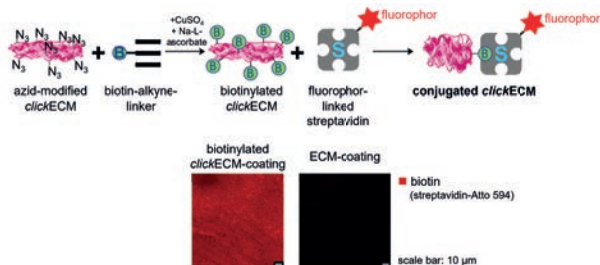


Fig. 2: Top scheme: Biotinylation of *click*ECM. Figure below: Successful conjugation of the *click*ECM azides with alkyne-functional biotin molecules (left image) demonstrated by coupling the biotin groups with a streptavidin-coupled fluorophore (ATTO 594-streptavidin, shown in red). Unmodified ECM coatings served as controls and showed no signal (right image). Microscope settings were kept identical for all images to ensure direct comparability of fluorescence intensities.

Methacrylated biomaterials for 3D bioprinting of personalized cartilage and tendon implants

Pinar Koca, Alexander Southan, Günter Tovar



Tendon, ligament, and cartilage injuries due to aging or athletic injuries are among the most common health problems worldwide and are underestimated contributors to long-term disability, reduced quality of life, and increased health costs. While surgical and non-surgical approaches exist, they have relatively long recovery times, fail to restore biological and mechanical functions of native tissues, and may cause donor-site-related problems due to a foreign body reaction.

Tissue engineering through the optimal combination of biomaterials, cells, and 3D bioprinting can address these challenges associated with biocompatibility, functionality, and morbidity and overcome the inadequacy of hydrogel scaffolds in clinical trials by mimicking the native extracellular environment of orthopedic soft tissues. To mimic the biochemical and mechanical properties of healthy cartilage and tendon structure, 3D bioprintable scaffolds based on methacrylated ECM-derived biomaterials are aimed to design.

These modified biomaterials provide flexibility in tailoring the stiffness of the hydrogel scaffolds via photopolymerization technique and shows printable properties that can allow to design and produce patient-specific temporally and spatially controlled multi-layered hydrogel scaffolds.

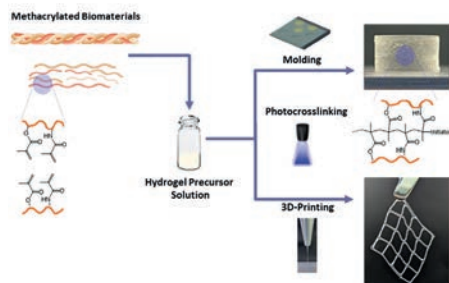


Fig. 1: Production of photocrosslinkable and 3D bioprintable methacrylated ECM-derived biomaterials for hydrogel scaffolds.

Collaboration: Fraunhofer Institute for Interfacial Engineering and Biotechnology IGB, Stuttgart; Viscofan BioEngineering, Weinheim, Germany; Institute for Complex Molecular Systems, Eindhoven University of Technology, Eindhoven, Netherlands; CELLINK AB, Gothenburg, Sweden; NanoBioCel Group, Laboratory of Pharmaceuticals, University of the Basque Country (UPV/EHU), Vitoria-Gasteiz, Spain; Leitat Technological Center, Barcelona, Spain; Football Club Barcelona, Medical Department, Barcelona, Spain; Osteoarthritis Foundation International OAFI, Barcelona, Spain; GradoCell S.L., Madrid, Spain; Cambridge Nanomaterial Technologies Ltd, Cambridge, UK

Funding: This project has received funding from the European Union's Horizon 2020 research and innovation framework programme under the Grant Agreement #952981. Website: <https://triankle.eu>

Physical and chemical cross-linking of gelatin-methacryloyl as scaffold for articular cartilage equivalents

Lisa Rebers, Alexander Southan, Kirsten Borchers, Günter Tovar

Articular cartilage appears simple since it consists only of chondrocytes and extracellular matrix (ECM). Up to now, the zonal structure has hardly been considered in the treatment of cartilage defects, although it is known to be essential for the material properties of cartilage. Thus, there is, a considerable need for research to develop methods for creating zonally structured cartilage equivalents by adapting biopolymer-based biomaterials.

Gelatin hydrogels are investigated as biomaterials because their collagen origin and high water content is similar to the extracellular matrix. Gelatin methacryloylate (GM) derivatives are investigated, which contain chemical cross-linkable C=C double bonds. The GM polymers can be covalently cross-

linked by radicals, for example in the presence of a irradiated photoinitiator. The aim of this research was the systematic investigation of GM synthesis, GM solutions and its cross-linking to hydrogels to select suitable GM derivatives for the construction of a zonally structured hydrogel as articular cartilage equivalent.

Different GM derivatives of gelatin type A (G_A) and gelatin type B (G_B) with different standard viscosities and almost identical Bloom values were compared. [1] It could be shown that the degrees of modification of the G_A and G_B derivatives were comparable. In contrast to this, significant differences between both gelatin types were found in the standard viscosity and in the storage modules of the hydrogels of

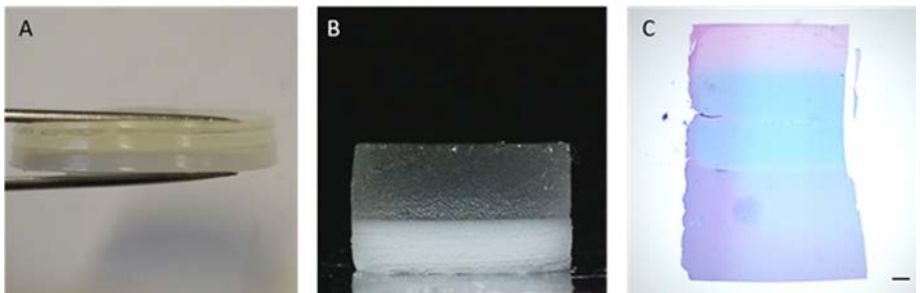


Fig. 1: Zonal hydrogels directly after preparation in the mold (A), cut sample for compression testing and cell encapsulation (B). In A and B the hyaluronic acid methacryloyl containing layer were opaque, while the other two layers were nearly transparent. A representative Alcian Blue-Nuclear Fast Red stained slice of zonal hydrogels is shown in C (scale bar = 500 μ m). The three layers could be differentiated by different staining.

the low-modified derivatives. These differences were attributed to the different standard viscosities of the raw materials, whereby a higher standard viscosity was linked with a higher storage modulus.

To further solidify GM hydrogels, sequential GM cross-linking, whereby, GM hydrogel precursor solutions are cooled prior to chemical crosslinking, was investigated. We showed that the compressive strength of obviously non-gelling hydrogel precursor solutions was increased by sequential cross-linking. [2] Further investigations showed that sequential crosslinking of the available double bonds lead to a lower double bond turnover in the resulting hydrogels than purely chemical cross-linking. [3] The solidifying effect of sequential GM crosslinking was attributed to the conformational change of the GM polymers during cooling prior to chemical cross-linking and the associated order.

The sequentially cross-linked GM hydrogels were then investigated for their suitability as scaffolding structure in zonal articular cartilage tissue engineering. Biomimetic hydrogel compositions consisting of GM, methacryloylated hyaluronic acid and methacryloylated chondroitin sulfate were investigated to generate a GM-based hydrogel with a biomimetic glycosaminoglycan gradients. Chondrocytes encapsulated in zonal and pure GM hydrogels synthesized cartilage-specific ECM. The zonal hydrogels studied could thus be further investigated as scaffolds for articular cartilage tissue engineering.

Publications: [1] Sewald, L., Claaßen, C., Götz, T., Claaßen, M. H., Truffault, V., Tovar, G. E. M., Southan, A., Borchers, K. (2018) Beyond the Modification Degree: Impact of Raw Material on Physicochemical Properties of Gelatin Type A and Type B, *Macromolecular Bioscience*, 18(12), 1800167–1800178. <https://doi.org/10.1002/mabi.201800168>
[2] Rebers, L., Granse, T., Tovar, G. E. M., Southan, A., Borchers, K. (2019) Physical Interactions Strengthen Chemical Gelatin Methacryloyl Gels, *Gels*, 5(1), 4–17. <https://doi.org/10.3390/gels5010004>
[3] Rebers, L.*, Reichsöllner, R.*, Regett, S., Tovar, G. E. M., Borchers, K., Baudis, S., Southan, A. (2021) Differentiation of Physical and Chemical Cross-Linking in Gelatin Methacryloyl Hydrogels, *Scientific Reports*, 11, 3256–3267 (*contributed equally). <https://doi.org/10.1038/s41598-021-82393-z>

Collaboration: Fraunhofer Institute for Interfacial Engineering and Biotechnology IGB, Stuttgart; Christian Doppler Laboratory for Advanced Polymers for Biomaterials and 3D Printing, Institute of Applied Synthetic Chemistry, TU Wien, Vienna, Austria

Funding: PhD scholarship of the Evonik Foundation

Development of a bio-based particulate drug delivery system for nose-to-brain transport of mAbs

Lena Marie Spindler,
Carmen Gruber-Traub, Günter Tovar



This doctoral thesis dealt with the development and characterization of bio-based particulate formulations for drug delivery in the olfactory cleft. The olfactory mucosa is directly connected to the brain and central nervous system via the olfactory nerve [1]. Intranasal drug delivery is an innovative route, especially for macromolecules, which allows bypassing the blood-brain barrier by transport along these nerves. The so-called nose-to-brain transport is therefore currently of particular interest for the therapy of neurological diseases with monoclonal antibodies (mAbs).

In *ex vivo* porcine olfactory mucosa, polylactide-co-glycolide (PLGA) nanoparticles (80 nm, 175 nm, 520 nm)

showed size- and time-dependent uptake [1]. It was determined that 520 nm PLGA particles associated with cell nuclei and neurofilaments within 15 min (Fig. 1 B,C), which could enable nose-to-brain transport as well as direct targeting [2] (Fig. 1 D). In comparison, chitosan-encapsulation of PLGA NPs via spray-drying even increased the uptake, which was attributed to chitosan to open tight junctions in the olfactory epithelium, allowing improving particle uptake through paracellular transport [1]. The opening of tight junctions by interaction with chitosan was demonstrated for the first time in olfactory tissue using immunohistochemical staining of the protein *Zonula Occludens 1* (ZO-1).

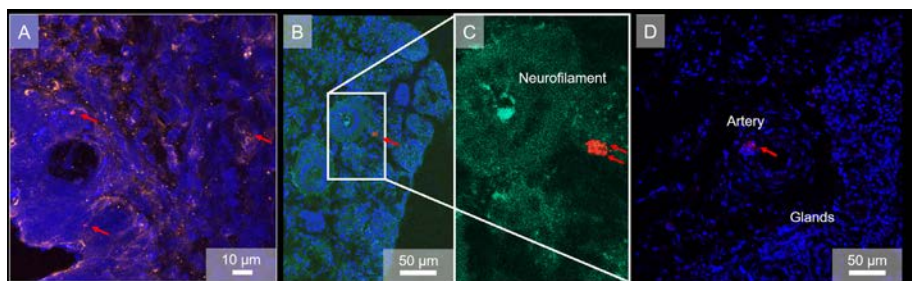


Fig. 1: Confocal laser scanning images (LSM) of cross-sections from porcine olfactory mucosa explants 15 min post particle application to the *apical* side. Blue: cell nuclei, DAPI. Red: polylactide-co-glycolide (PLGA) nanoparticles (520 nm), Lumogen. Cyan: Neurofilament heavy protein H, Fluorescein isothiocyanat. A: Epithelial and basal cell layer of porcine olfactory mucosa explants with 520 nm particles applied to the apical side. B: Co-localization of 520 nm nanoparticles with neuronal fibers. C: Enlargement of B. D: Targeting of CD20 (cluster of differentiation) in, e.g., blood vessels via ocrelizumab-functionalized particles.

At 100°C spray drying inlet temperature, particles with smooth surface, monomodal particle size distribution and mean diameters of 69±9 nm could be produced. The process parameters optimized in this dissertation enabled high particle yields over 60% and continuous production over 40 min. The mAb ocrelizumab was encapsulated in chitosan for the first time in this dissertation; a high encapsulation efficiency of over 80% was achieved for loadings up to 15 wt% using spray drying. Ocrelizumab remained structurally largely intact. The glass transition temperature of the developed particles was 35°C, confirming their storage stability over five weeks at room temperature. Dissolution tests *in vitro* showed no burst release. After 360 h, 84±5% ocrelizumab was released successfully.

To be able to fix the developed particle formulation to the olfactory cleft, native and tyramine-modified hyaluronic acid solutions (HA, HA-Tyr) were investigated as a possible coating on mucosa. The physiological conditions of the nose favored their spreading [3].

Overall, in this Ph.D. thesis a chitosan-based particulate drug formulation using spray drying was successfully developed, which enables structurally intact encapsulation of monoclonal antibodies. Controlled release over 15 days was achieved for the therapeutic antibody ocrelizumab, and the matrix material chitosan caused the opening of tight junctions in the porcine olfactory mucosa. This resulted in enhanced uptake in the olfactory epithelium, which is consistent with overcoming this biological barrier and highlights the

suitability of the developed particles for intranasal delivery.

Publications: [1] Spindler, L. M., Feuerhake, A., Ladel, S., Gunday, C., Flamm, J., Gunday-Tureli, N., Tureli, E., Tovar, G. E. M., Schindowski, K., Gruber-Traub, C. (2021) Nano-in-Micro-Particles Consisting of PLGA Nanoparticles Embedded in Chitosan Microparticles via Spray-Drying Enhances Their Uptake in the Olfactory Mucosa, *Frontiers in Pharmacology*, 12, 19. <https://doi.org/10.3389/fphar.2021.732954>

[2] Tschiche*, H. R., Bierkandt, F. S., Creutzenberg, O., Fessard, V., Franz, R., Greiner, R., Gruber-Traub, C., Haas, K. H., Haase, A., Hartwig, A., Hesse, B., Hund Rinke, K., Iden, P., Kromer, C., Löschner, K., Mutz, D., Rakow, A., Rasmussen, K., Rauscher, H., Richter, H., Schoon, J., Schmid, O., Som, C., Spindler, L. M., Tovar, G. E. M., Westerhoff, P., Wohlleben, W., Luch, A., Laux, P. (2022) The release and toxicological aspects of nanomaterials in various scenarios: Challenges and way forward, *Nanoimpact*, 28, 100416. <https://doi.org/10.1016/j.impact.2022.100416>

[3] Spindler, L. M., Serpetsi, S., Flamm, J., Feuerhake, A., Böhrer, L., Pravda, M., Borchers, K., Tovar*, G. E. M., Schindowski, K., Gruber-Traub*, C. (2022) Hyaluronate Spreading Validates Mucin-Agarose Analogs as Test System to Replace Porcine Nasal Mucosa Explants – an Experimental and Theoretical Investigation, *Colloid and Surfaces B: Biointerfaces*, 112689bbb. <https://doi.org/10.1016/j.colsurfb.2022.112689>

Collaboration: C. Gruber-Traub, M. Müller, A. Weber, K. Borchers, P. Loskill and A. Burger-Kentscher – Fraunhofer Institute for Interfacial Engineering and Biotechnology IGB, Stuttgart; K. Schindowski-Zimmermann, S. Ladel and F. Maigler – Institute for Applied Biotechnology, Biberach University of Applied Science, Biberach; N. Gunday-Tureli, E. Tureli, C. Gunday – MyBiotech GmbH, Überherrn, Germany; M. Pravda – Contipro a.s., Dolní Dobrouč, Czech Republic; S. Serpetsi – Chemical Process & Energy Resources Institute, Centre for Research and Technology Hellas, Thessaloniki, Greece; M. Calamai and C. Capitini – LENS, European Laboratory for Non-Linear Spectroscopy, University of Florence, Florence, Italy

Funding: PhD scholarship of the Studienstiftung des deutschen Volkes e. V.; European Union's Horizon 2020 research and innovation programme under grant agreement No. 721098 (www.n2b-patch.eu)

Bio2Brain: Bio-based hydrogels as drug delivery systems for the intranasal transmucosal delivery of biopharmaceuticals

Erik Taylor, Beatrice Di Lelio,
Dr. Carmen Gruber-Traub, Günter Tovar

There is a critical need for development of drug delivery technologies for efficient administration of large biopharmaceuticals for treatment of central nervous system diseases. The intranasal drug delivery route is of specific interest for bypassing the Blood-Brain-Barrier. Hydrogel delivery systems are promising, due to their tunable chemical, physical, and bioactive properties.

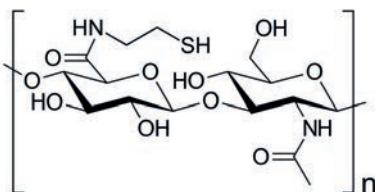


Fig. 1: Structure of cysteamine-modified hyaluronic acid.

Therefore, hyaluronic acid (HA) hydrogels have been modified with cysteamine to enable enhanced mucoadhesion through disulfide bond formation between the thiolated hydrogel and cysteine regimes present in mucins. To date, synthesis of HA-cysteamine derivatives is undergoing continued optimization to enable precise control over degree of substitution. Hydrogels are characterized via FT-IR, $^1\text{H-NMR}$, elemental analysis, and determination of free-thiol content. The mucoadhesive properties of hydrogels are determined via rheology and contact angle

measurements, using mucin-agarose substrates as imitation mucosa. Molecular dynamics modeling has been used to calculate the binding free energy of HA-mucin systems.

In ongoing work, the mucoadhesive properties of HA derivatives will be further characterized using ex vivo porcine mucosa substrates. Furthermore, the HA-cysteamine hydrogels will be combined with particle systems developed by collaborators, and the drug release characteristics of the hydrogel-particle system will be determined.

Collaboration: Fraunhofer Institute for Interfacial Engineering and Biotechnology IGB, Stuttgart

Funding: European Union's Horizon 2020 research and innovation programme under the Marie Skłodowska-Curie grant agreement No 956977

6 CLEAN WATER AND SANITATION





Energetic and economic viability of active atmospheric water generation technologies

Julius Potyka, Antoine Dalibard, Günter Tovar

Water scarcity is an increasing global and systematic problem worldwide in regions with low ground water availability and large distances to shores. Atmospheric water generation (AWG) technologies are an innovative solution to fight drinking water shortages, since atmospheric water vapour is a readily available resource even in arid areas, but have the downside of a high specific energy expenditure.

To assess the suitability of AWG technologies as an alternative drinking water supply regarding their energetic and economic efficiency, thermodynamic models of different AWG systems are used for a comparative analysis. A location analysis model is developed evaluating the performance based on

representative weather data of temperature, pressure and relative humidity. Seawater desalination at the nearest shore and transport to the location is used as a benchmark for the economic evaluation. Results show that active AWG systems can function as an alternative as long as the water usage location is relatively far away from shore or other water rich regions and proportionally low amounts of overall water are required for that region. Sorptive systems have an energetic efficiency advantage over cooling condensation systems but require a higher degree of process and plant design R&D.

Collaboration: Fraunhofer Institute for Interfacial Engineering and Biotechnology IGB, Stuttgart

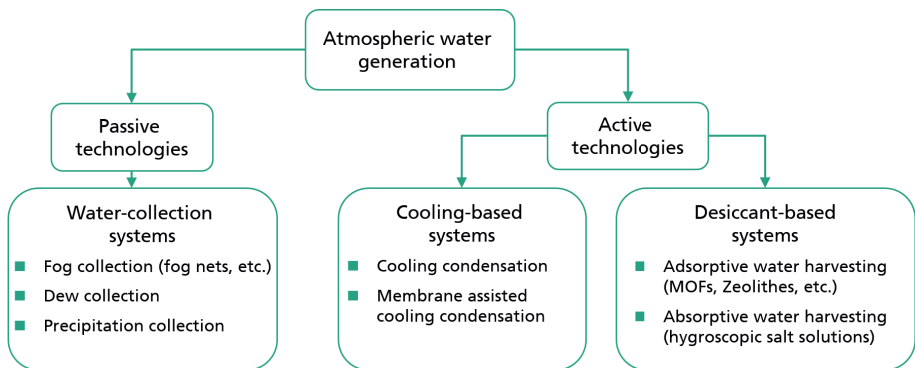


Fig. 1: Overview of different AWG technologies divided into their respective categories.



Hydrogels as functional coatings for sensor applications

Anastasia Tsianaka, Alexander Southan, Günter Tovar

Analytics of mixtures of different substances play a crucial role in many environmental or industrial applications. Determination of analyte concentrations, such as pharmaceutical compounds present in water bodies or reactants during industrial processes, is crucial. The use of methods that require simple instrumentation and deliver prompt results is advantageous. Optical sensors are devices that fulfill these requirements.

Optical sensors based on Silicon, combined with a functional coating which can interact with analytes can monitor refractive index changes caused by the presence of said analytes in aqueous solutions. Hydrogels, polymer networks which enable analyte enrichment due to their swelling properties, are suitable functional layers. Through introduction of functional groups in the polymer network, adsorption of specific analytes is enabled. This project is focused on the characterization of functionalized hydrogels for the adsorption of pharmaceutical compounds such as diclofenac and metoprolol present in aqueous solutions, as well as on the deposition of these functional layers on sensor surfaces. A microfluidics-based coating method that allows a spatial control of the hydrogel deposition is to be developed to ultimately obtain fully functional optical sensors.

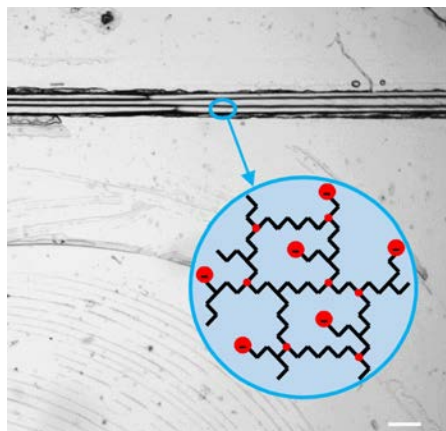
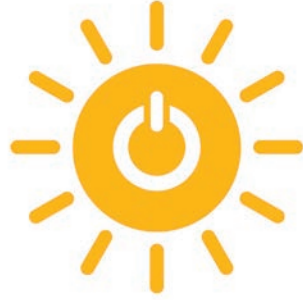


Fig. 1: Hydrogel coating in a 150 μm wide microfluidic channel (scale: 250 μm). The hydrogel contains negatively charged functional groups for the adsorption of the pharmaceutical compound metoprolol.

Collaboration: Manfred Berroth, Wolfgang Vogel, Niklas Hoppe and Christian Schweikert, Institute of Electrical and Optical Communications Engineering (INT), University of Stuttgart; Fraunhofer Institute for Interfacial Engineering and Biotechnology IGB, Stuttgart

Funding: German Research Foundation (DFG), Funding code: TO 211/4-1

7 AFFORDABLE AND CLEAN ENERGY





Numerical investigation of hydrogen plasma from the Duo-Plasmaline in a magnetic field

Stefan Merli, Andreas Schulz, Matthias Walker

The influence of magnetic fields on the properties of hydrogen plasma from the Duo-Plasmaline was simulated with Comsol Multiphysics. The model solves the plasma transport equations self-consistently with the microwave electric field and a set of 42 plasma reactions with 14 species. A constant and homogeneous magnetic field B was added in parallel or perpendicular orientation to the Duo-Plasmaline axis. The magnetic field affects the plasma shape and heating mechanism due to a reduction of the electron mobility and diffusivity perpendicular to B . Therefore, the perpendicular density profiles are more peaked towards the plasma source with increasing B . The electron conductivity perpendicular to B decreases by 2 orders of magnitude at 1 T, which leads to a reduced absorption of the microwave electric field and a lower perpendicular heating efficiency. However, the heating mechanism changes from the absorption of the perpendicular field component to the parallel component, which is not influenced by B . This leads to efficient plasma heating even at 1 T. The conductivity has a maximum at 87.5 mT due to electron cyclotron resonance (ECR), which makes the microwave heating most efficient leading to high electron temperatures and densities (Fig. 1). The qualitative simulation results were in good agreement with experimental observations.

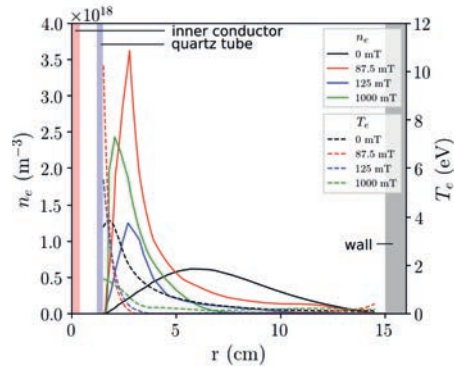


Fig. 1: Radial profiles of the electron density and temperature for 20 Pa, 2000 W microwave power and different magnetic flux densities.

Collaboration: Y. Kathage, S. Hanke, C. Day, ITEP, Karlsruhe Institute of Technology (KIT), Karlsruhe; K. M. Baumgärtner, M. Gorath, Muegge GmbH, Reichelsheim

Funding: This work has been carried out within the framework of the EUROfusion Consortium under the Work Package TFV (Tritium, Matter Injection and Vacuum) and has received funding from the Euratom research and training programme 2014–2018 and 2019–2020 under grant agreement No 633053. The views and opinions expressed herein do not necessarily reflect those of the European Commission.



Experimental investigation of hydrogen plasma from the Duo-Plasmaline in a magnetic field

Stefan Merli, Andreas Schulz, Matthias Walker

The influence of a magnetic field on hydrogen plasmas from the Duo-Plasmaline has been investigated in the experiment FLIPS. FLIPS consists of a vacuum chamber equipped with many diagnostic ports and a coil system, which creates a homogeneous B-field of up to 250 mT. The Duo-Plasmaline was installed in parallel or perpendicular orientation to the B-field. The plasma was investigated with regard to its ignitability and stability at different microwave power P , pressure p and magnetic flux density B .

microwave heating was most efficient because of the electron cyclotron resonance heating (ECRH). The influence of the B-field decreases with increasing p due to the higher collision frequency. At $B > 100$ mT, the absorption of the microwave decreases due to the lower conductivity perpendicular to B so that more microwave power is needed for ignition. For a high B/p ratio the plasma is “trapped” along magnetic field lines and extends beyond the actual plasma source, creating a “plasma tube” in parallel orientation or a “plasma wall” in perpendicular orientation (Fig. 1).

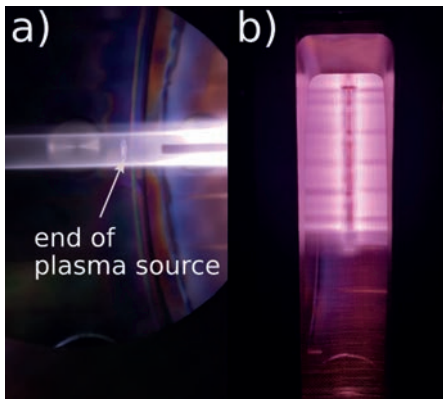


Fig. 1: Different structures of MEL produced from rapeseed oil depending on the employed microorganisms.

The experimental observations agreed well with results from the simulations.

Collaboration: Y. Kathage, S. Hanke, C. Day, ITEP, Karlsruhe Institute of Technology (KIT), Karlsruhe; K. M. Baumgärtner, M. Gorath, Muegge GmbH, Reichelsheim

Funding: This work has been carried out within the framework of the EUROfusion Consortium under the Work Package TFV (Tritium, Matter Injection and Vacuum) and has received funding from the Euratom research and training programme 2014–2018 and 2019–2020 under grant agreement No 633053. The views and opinions expressed herein do not necessarily reflect those of the European Commission.

At low B around 50 mT, the plasma had an increased ignitability compared to without B , especially at low pressure due to the reduced diffusion of the electrons perpendicular to B . At 87.5 mT the



Design of a focusing horn antenna for a correlation ECE system for W7-X

Burkhard Plaum, Achim Zeidler

For a new correlation ECE (electron cyclotron emission) system for the stellarator W7-X, a focusing antenna for frequencies around 138 GHz was required. While smooth walled Gaussian horn antennas usually have the waist inside the horn or directly at the aperture, moving the waist outside of the horn requires a non-trivial mode mixture in the aperture. Furthermore, such antennas are usually quite large and have a limited bandwidth. The PROFUSION optimizer takes the input radius, geometrical limits and the desired output field pattern as parameters and writes out the radius as a function of the axial coordinate. The solution has a clear focus starting at a distance of about 200 mm from the aperture (see Fig. 1 top). The antenna has a length of about 320 mm and was manufactured at IGVP in split block technology (see Fig. 2), where the geometry is milled into aluminium blocks, which are then screwed together. This technology allows to integrate a transition from the rectangular input waveguide to the circular cross section of the antenna. The principal behaviour could be verified experimentally.

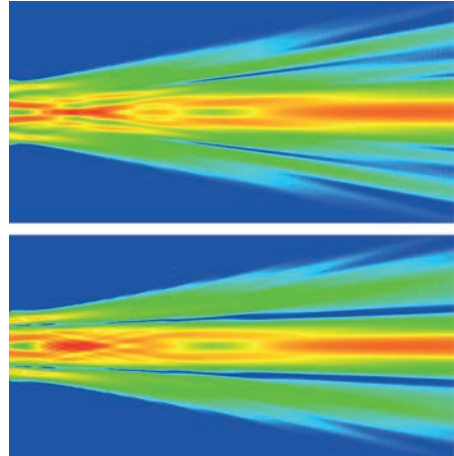


Fig. 1: Horizontal (top) and vertical (bottom) profile of the calculated radiated beam. Size of the field is 400x200 mm, logarithmic plot, 30 dB dynamic range.

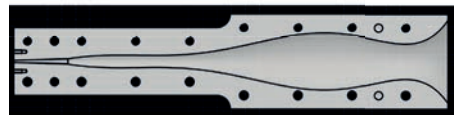
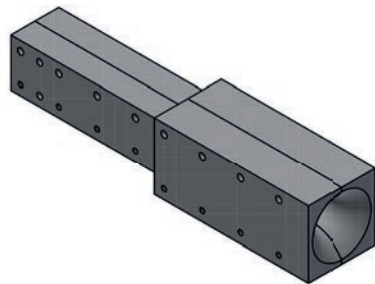


Fig. 2: Blueprints of the antenna.

Collaboration: G. Weir, M. Hirsch, Max Planck Institute for Plasma Physics (IPP), Greifswald

Funding: Max Planck Institute for Plasma Physics (IPP), Greifswald



Generation of a homogeneous microwave field for an ECEI detector array

Burkhard Plaum

For an ECE-imaging system at ASDEX-Uprade, a linear detector array is used. It consists of mixers, which need to be illuminated with a local oscillator (LO-) signal in the range of 75 to 105 GHz. To ensure equal signal levels for all detectors along the width of 340 mm special beam shaping optic are required.

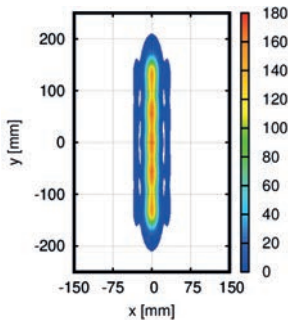


Fig. 1: Field at 90 GHz at the detector array.

A first variant consists of a rectangular waveguide taper, which enlarges the WR10 waveguide to a size of 10 mm × 30 mm. It is followed by an optical system consisting of two horizontally and two vertically focusing lenses, which realize the required magnification factors in a confocal configuration. The positions and focal lengths can be calculated analytically assuming a thin lens approximation. Fig. 1 shows the field at 90 GHz at the detector array, Fig. 2 shows the power distribution at the detector array for 75, 90 and 105 GHz.

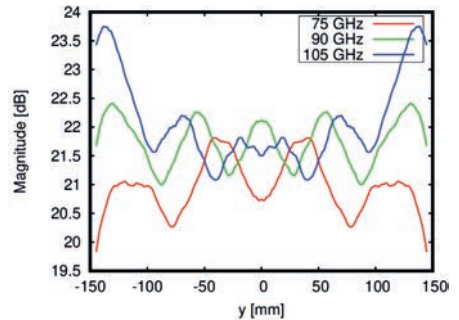


Fig. 2: Power distribution at the detector array for 75, 90 and 105 GHz.

It was found, that this approach requires very thick lenses, which produce noticeable distortions and are difficult to simulate within an optimizer loop. Furthermore it requires a lot of space. Therefore, a more compact alternative based on waveguide power splitters and tapers is investigated.

Collaboration: B. Vanovac, W. Suttrop, Max Planck Institute for Plasma Physics (IPP), Garching

Funding: Max Planck Institute for Plasma Physics (IPP), Garching



Development of diffraction gratings for advanced ECRH scenarios

Burkhard Plaum

The development of specialized diffraction gratings continued in 2020. They are used to redirect the remaining power of an ECRH beam back into the plasma for a second heating pass in the case of an imperfect absorption, e.g. when heating at higher harmonics. The main focus was the support of gratings, which span multiple reflection tiles. In a stellarator, the tiles are smaller than typical beam diameters and have non-trivial shapes. A grating, which spans multiple tiles, must be optimized in a single run to avoid phase discontinuities at the interfaces between the tiles. This requires support of a base surface, which is given numerically. Gaps and discontinuities at the tile boundaries are smoothed by a CAD software. From the surface, which is

given on a cartesian grid, the normal vectors are calculated numerically and the local k-vectors are calculated from the incident beam. This allows to obtain the local groove direction at any point of the surface and a coherent layout of grooves can be obtained for the whole reflector.

Collaboration: T. Stange, M. Schubert, Max Planck Institute for Plasma Physics (IPP), Garching and Greifswald

Funding: Max Planck Institute for Plasma Physics (IPP), Garching and Greifswald

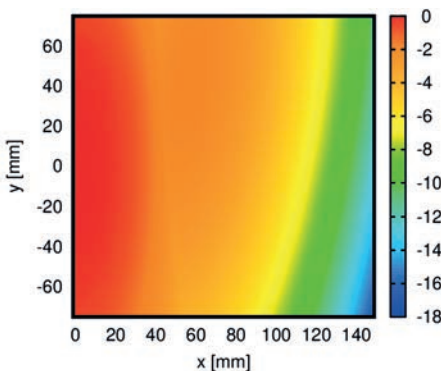


Fig. 1: Complex base shape of a reflector.

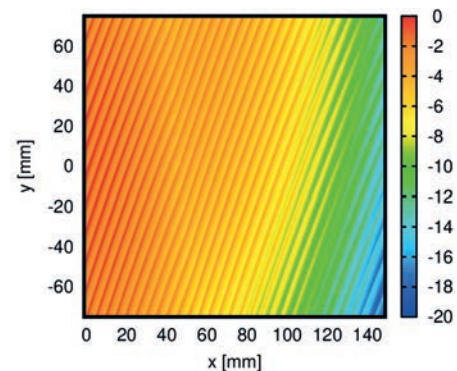


Fig. 2: Grating imposed on the reflector.



Simulation of the microwave optics for the first plasma in ITER

Burkhard Plaum

For the first plasma operation of ITER, the machine will run with a limited set of components installed. In particular the ECRH launcher in the equatorial plane will be missing. Therefore, a dedicated optic is planned, which allows plasma breakdown with microwave beams launched from the upper launcher. 3 beams from the upper row (U-beams) are directed via an ellipsoidal mirror (UA) through the resonance into a dedicated beam dump, which is installed in the port foreseen for the equatorial launcher. 4 beams from the lower row of the upper launcher (L-beams) are directed by a single ellipsoid mirror (LA) and 4 individual hyperboloidal mirrors (LB) to the same beam dump.

The whole system is simulated with PROFUSION. Several tools were written and adapted for the requirements of this task. The results are compared with raytracing calculations. Different issues, like the beam truncation due to the limited size of the mirror UA, are investigated in detail. Fig. 1 shows the beam footprint of the U1 beam on the mirror UA. Fig. 2 shows the spillover power behind the mirror, which is used to estimate the heat load on the vessel wall.

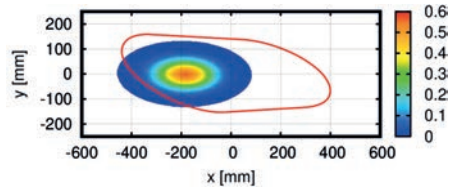


Fig. 1: Field of the beam U1 on the mirror UA (contour in red).

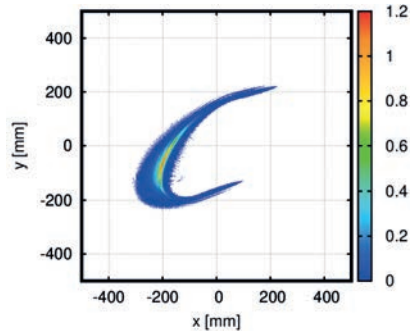


Fig. 2: Spillover field propagated behind the mirror to investigate the heat load on the vessel wall.

Publication: Plaum, B., Preynas, M., Choe, M. (2022) Calculations for the optical system for the first ITER plasma, Proc of 21st joint workshop on electron cyclotron emission (ECE) and electron cyclotron resonance heating (ECRH), accepted

Collaboration: M. Preynas, M. Henderson, ITER Organization, St Paul Lez Durance Cedex, France

Funding: ITER Organization, Service contract 43-2080



Calculations for the EBW-launcher for MAST Upgrade

Burkhard Plaum

IGVP supports the design of microwave launchers for EBW heating for the MAST Upgrade experiment. In the initial version, the launcher consisted of a fixed mirror and a steering mirror to enable injection in both co- and counter-current directions. Both mirrors were focusing, which is a problem because the focal length of a steerable mirror depends on the steering position. The mirror surface was designed for one position and the beams for other steering positions were calculated with PROFUSION. From the field after the last mirror, the ellipse radii were obtained. These were compared with the design values obtained with the formulas for Gaussian beams. As an example, the radii of the beam ellipse of the left midplane launcher are plotted as a function of the propagation distance. The steering mirror was designed for co-current injection. When operating in co-current injection, we see a perfect agreement of the ellipse radii with the design values (Fig. 1). When operating in counter injection, the beam radii change significantly (Fig. 2). A revised design with a flat steering mirror is currently under investigation.

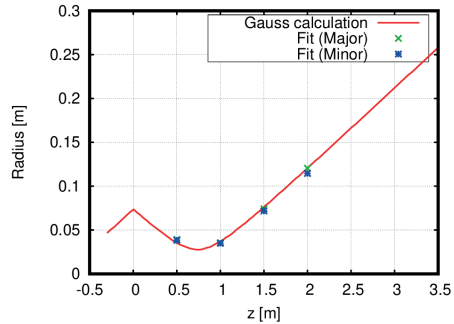


Fig. 1: Radiated field of the left midplane launcher (designed for co-injection, operating in co-injection).

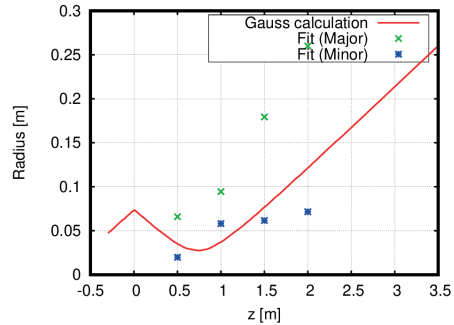


Fig. 2: Radiated field of the left midplane launcher (designed for co-injection, operating in counter-injection).

Collaboration: S. Freethy, M. Henderson, J. Allen, M. Lennholm, Culham Centre for Fusion Energy, UK

Funding: UK Atomic Energy Authority



Design of a hole array for use as a dual frequency power monitor for high power transmission lines

Burkhard Plaum, Lina Wang

Power monitors are essential for high power transmission lines. They can be used for diagnosing problems and to switch off the sources in cases of a malfunction. They need to extract a small portion of the megawatt beam for analysis with low power equipment. In this study, hole arrays are integrated into a miterbend mirror, while the diagnostic signal is coupled to a fundamental mode waveguide below the mirror surface. By using hole diameters below cutoff, attenuations of 60 dB can easily be achieved. In order to work at two frequencies (105 and 140 GHz), the hole sizes need to be optimized such that the main lobe at 105 GHz has the same direction (45°) as a side lobe at 140 GHz. Another goal is the sensitivity for higher order modes, which must be small in order to get reliable power values. Numerous optimizations with different methods and cost functions were done. A calculated example for

optimized antenna patterns is shown in Fig. 1, where we see a strong sensitivity lobe at 45° for both frequencies and polarizations.

An experimental characterization will be done in 2023.

Funding: University of Electronic Science and Technology of China, School of Electronic Science and Engineering, Chengdu, China

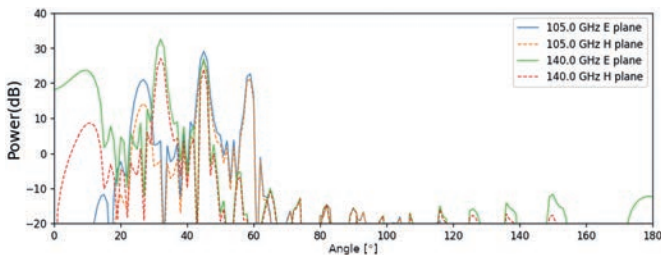


Fig. 1: Calculated antenna diagram.



PROFUSION code development

Burkhard Plaum

The PROFUSION code (Programs for multimode analysis, simulation and optimization) is constantly extended and enhanced as requested by other projects. In 2020 the development focused on the accurate calculation of the reflection of microwave beams on metallic mirrors using a physical optics method, which is used for calculating the optical setup for the ITER first plasma. It works by calculating the currents in the mirror surface from the incident field on a regular cartesian grid in mirror coordinates. These current elements are then treated as Huygens-sources and the reflected field is calculated by a simple summation. The algorithm, which includes 4 nested loops, is parallelized on multi-core architectures. The physical optics method allows to calculate higher order effects like mode conversion or the generation of cross polarized field components (see Fig. 2).

Further developments were:

- A frontend for the optimization of waveguide tapers with a rectangular cross section
- Tools for the simple tracking the polarization vectors along a series of mirrors
- A tool for generating discretized mirror surfaces from geometrical descriptions (cylinder, ellipsoid or hyperboloid) for using with the physical optics algorithm

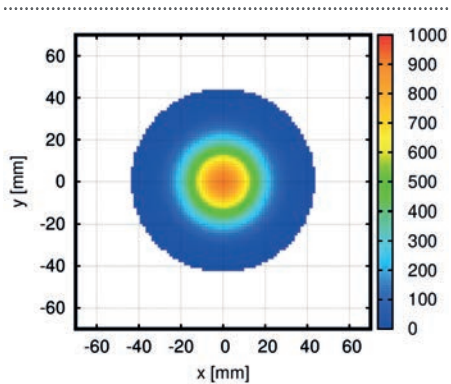


Fig. 1: Gaussian beam reflected by an ellipsoidal mirror (co-polarization).

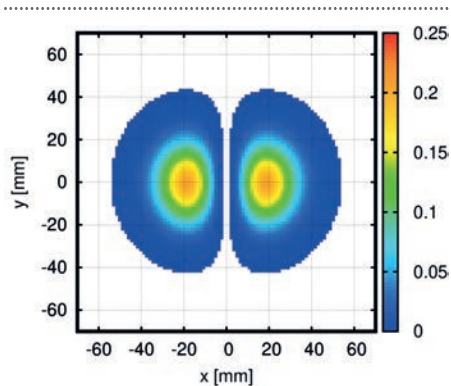


Fig. 2: Gaussian beam reflected by an ellipsoidal mirror (cross-polarization).



Microwave absorbing layer materials for fusion reactors

Andreas Hentrich, Carsten Lechte, Burkhard Plaum, Günter Tovar

An issue which was long neglected in the field of nuclear fusion is how to handle the stray radiation induced by imperfect absorption of heating power. To overcome this problem, new microwave absorbing coatings were developed in collaboration with the IFKK and on behalf of ITER.

Adding a high power absorber to a fusion reactor comes with a lot of constraints, which render classical microwave absorbers useless. So several ceramic layers were investigated regarding their thickness, incidence angle and polarization dependent absorption properties to achieve resonant absorption. The aim there is to trap the microwaves inside the absorbing layer by changing the layer parameters in a way that destructive interference happens. A complementary model was designed to generalize and understand the observed behavior. The combination of model and measurements also allows for the identification of the material parameters.

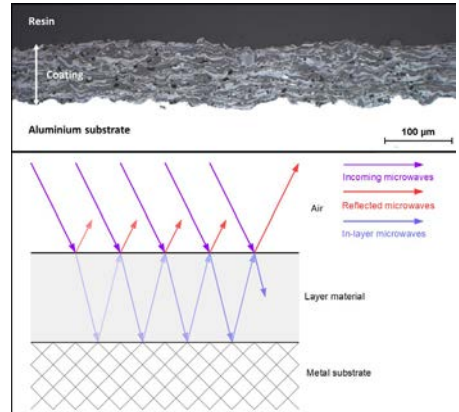


Fig. 1: The upper part shows a microscopic cross section of the beam dump material, which will later be used in ITER. The lower one represents the same system in the context of the simulations showing the calculated plane waves.

The findings culminated now into a matrix formalism, which enables to accurately simulate every layered material system on a metal substrate. The theoretical results for multi-layer resonant absorbers are very promising and when they can be verified experimentally, it is possible to build almost ideal microwave absorbers for fusion devices by design.

Publications: Hentrich, A. et al. (2022) Resonant Atmospheric Plasma-Sprayed Ceramic Layers Effectively absorb Microwaves at 170GHz., *Journal of Infrared, Millimeter, and Terahertz Waves*, 43, 349–365, <https://doi.org/10.1007/s10762-022-00861-7>

Hentrich, A. (2022) Simulation and reflectivity measurements of the ITER first plasma beam dump material, EC-21 conference proceedings, accepted



Fullwave Doppler reflectometry simulations for ASDEX Upgrade

Carsten Lechte

Magnetically confined fusion plasmas with temperatures of 200 million Kelvin are plagued by turbulent fluctuations of important plasma parameters. Turbulence is a driver of particle and energy transport out of the magnetic confinement.

Doppler reflectometry is a microwave scattering diagnostic that is eminently suitable for hot plasmas: It is contactless, and the required frequencies result in useful spatial and temporal resolution. It measures the density fluctuation wavenumber spectrum and plasma flow velocity, which are important turbulence characteristics. Like RADAR, probing beams are emitted, but the interpretation of the scattered signal is not straightforward because of non-linear and multiple scattering. The IGVP fullwave code IPF-FD3D implements this as a *synthetic diagnostic*.

A new campaign was started at IPP Garching to collect extensive measurements and accompanying turbulence simulations. Our synthetic diagnostic then uses the turbulence simulation data to compute the synthetic Doppler reflectometry signal. The synthetic signal can then be compared directly to the experimental Doppler signal.

Fig. 1 shows the 2D computational grid, which covers the upper and outer quadrant of a poloidal/vertical slice of ASDEX

Upgrade. The beam is injected from the vacuum, propagates to the cutoff layer, and is scattered back into the antenna. Many different beams at different launch angles and different frequencies are combined with many different time slices of the plasma turbulence.

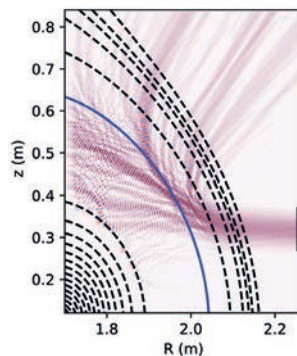


Fig. 1: Computational grid with plasma density contours (dashed) and wavefield (red-blue). The antenna is represented by the triangle on the right. The blue contour line is the cutoff density contour, where the wave is reflected and scattered into the upper right direction.

A typical set of resulting Doppler spectra is shown in Fig. 2: Each curve in the plot is the result of a single probing beam, and it is associated with one wavenumber k_{\perp} of the density fluctuations. Each curve also shows the spectral broadening and Doppler shift of its frequency. Higher wavenumbers have a lower spectral power, but a larger Doppler shift.

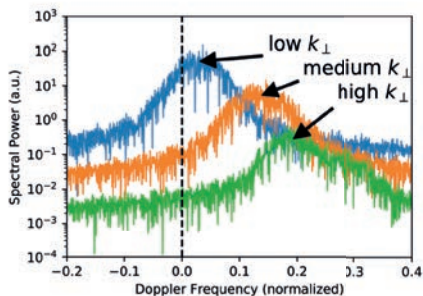


Fig. 2: Overlaid Doppler spectra for a selection of probed wavenumbers k_{\perp} . The abscissa shows the frequency Doppler shift of the signal, the ordinate is spectral power.

A direct comparison between experiment and turbulence simulations shows large discrepancies. A meaningful comparison is possible only after applying our synthetic diagnostic: Overall, the fullwave simulations show good agreement in the wavenumber spectra and radial correlation lengths compared with experimental results.

The non-trivial diagnostic effect is illustrated on Fig. 3: Input density fluctu-

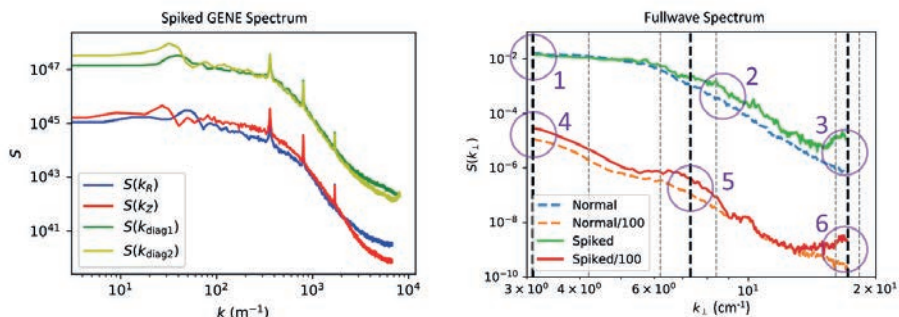


Fig. 3: 1D slices of the 2D wavenumber spectrum of the turbulent fluctuations used as input to the fullwave simulations with added spikes at 3 wavenumbers (left) and the resultant fullwave reconstruction of the spectra (right).

ations for the fullwave simulations were overlaid with 3 different single-wavenumber fluctuations (“spikes”, left) and put through the synthetic diagnostic. In the resulting wavenumber spectrum on the right (“Fullwave”), these input spikes are either smeared out (3,4,5,6), shifted to higher wavenumbers and smeared (2), or absent entirely (1).

Publications: [1] Lechte, C., Conway, G., Görler, T., Happel, T., and the ASDEX Upgrade Team (2020) Plasma Sci. Technol. 22 064006, <https://doi.org/10.1088/2058-6272/ab7ce8>

[2] Lechte, C., Happel, T., Höfler, K., Görler, T., Frank, A., Conway, G., and the ASDEX Upgrade Team (2022) Fullwave Doppler Reflectometry Simulations Coupled with GENE Plasma Turbulence Simulations. In Proceedings of the 15th International Reflectometry Workshop for fusion plasma diagnostics (IRW15)

Collaboration: Antonia Frank, Klara Höfler, Tim Happel, Max Planck Institute for Plasma Physics (IPP), Garching and Greifswald

Funding: Max Planck Institute for Plasma Physics (IPP), Garching and Greifswald

The simulations were performed on the national supercomputer HPE Apollo Hawk at the High Performance Computing Center Stuttgart (HLRS) under the grant number syntref/44034.

Optimisation of a broadband antenna for plasma positioning reflectometry

Johannes Lips, Carsten Lechte

The plasma position in a tokamak fusion device depends on internal plasma currents and therefore needs to be measured. A microwave reflectometer can be positioned in a gap in the blanket that constitutes the inner vessel wall.

The antenna needs to work for a large frequency range (30–60 GHz) and must form the beam in a way that avoids spurious reflections from the blanket installation. In addition, strong edge plasma turbulence will scatter much of the beam power away from the antenna, which for space reasons will be a monostatic design.

The radiation diagram was optimized using PROFUSION and the newly developed raytracing code R2P2. Several different amplitude distributions at the antenna mouth were analysed with raytracing and typical plasma and turbulence profiles at several representative frequencies within the

range. A Gaussian beam pattern had the optimal combination of high direct reflected power from the plasma and low sensitivity to spurious reflections on turbulence and blanket structures.

A prototype antenna was synthesized and compared experimentally with a standard cylindrical horn. The optimised horn performed well without the blanket structures, but the radiation pattern deteriorated when the mock-up blanket was present. This was in part because the optimisation process only looked at desirable radiation patterns on the antenna mouth, and did not include blanket effects.

Publications: [1] Lips, J. (2020) Antenna Optimization for Plasma Positioning Reflectometry in Blanket-Equipped Tokamaks, Master's thesis, Université de Lorraine and Universiteit Gent and Universität Stuttgart

Collaboration: Stéphane Heuraux, Institut Jean Lamour, Université de Lorraine, Nancy

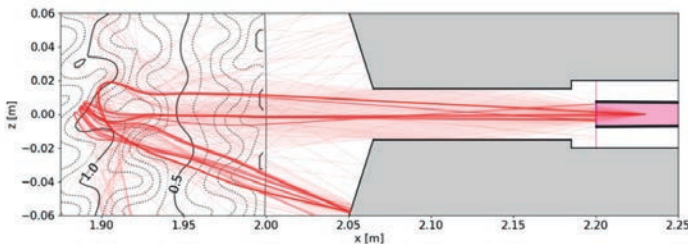


Fig. 1: Results of raytracing with R2P2 for a plasma with high levels of turbulent fluctuations: Rays are passing through the plasma, reflect on the wall, and pass through the plasma again before hitting the antenna (plot adapted from [1]).

Fullwave 3D simulations of an ICRF antenna interferometer

Carsten Lechte

ICRF plasma heating takes place at ion cyclotron frequencies, which in fusion plasmas are in the 20–100 MHz range. At these large wavelengths, the waves cannot propagate without plasma. Care has to be taken with the coupling of ICRF array antennas to the plasma edge. Information on plasma density in front of the antenna is given by interferometry. The interferometer in this case has a 45 cm long nearly vertical sight line from the bottom to the top of the ICRH antenna.

Since all material installations have to be outside the plasma confinement region, there is a steep plasma density gradient from the edge of the plasma ($6 \times 10^{19} \text{ m}^{-3}$, more than twice the cutoff density of the interferometer beam) to the antennas, where the density is basically zero. The beam sees a large transverse density gradient as it propagates (Fig. 1). Without that gradient, the received phase shift from the plasma would be simply proportional to the integral of the plasma density along the beam axis. The simulations are done to see what kind of phase information is actually seen at the receiving antenna.

First results show a strong asymmetry. The large plasma density on the left refracts and reflects the beam, sending the left part into the receiving antenna, which would usually not hit the antenna, overlaying its phase information

onto the central part of the beam. It is currently under investigation how to quantify these contributions.

Collaboration: Mariia Usoltceva, Max Planck Institute for Plasma Physics (IPP), Garching and Greifswald; Stéphane Heuraux, Institut Jean Lamour, Université de Lorraine, Nancy

Funding: Max Planck Institute for Plasma Physics (IPP), Garching and Greifswald

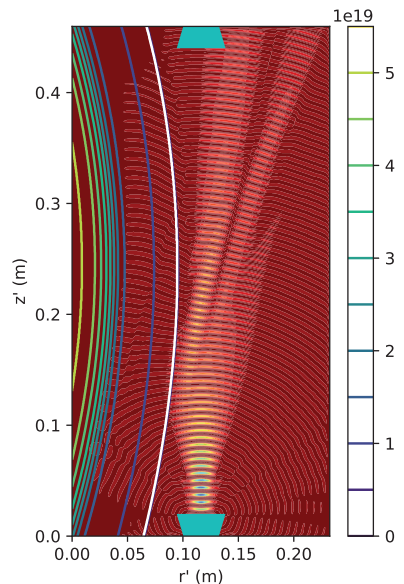


Fig. 1: Wave field in color with overlaid plasma density contours. The white contour corresponds to 10% of the maximum density in the plot. The sending antenna is at the bottom, the receiving antenna at the top (cyan trapezoids). Density is in m^{-3} . r' and z' are the tilted radial and vertical coordinates.



Fullwave 3D simulations of diffraction losses in a 170 GHz miterbend

Carsten Lechte, Rutai Chen

High power microwave transmission lines transport power over hundreds of meters at power densities surpassing 500 MW/m². For frequencies above 10 GHz, this still means using oversized waveguides, e.g. 50 mm diameter for 170 GHz. In these waveguides, only the fundamental mode is used, but higher order modes (HOMs) can be excited by misalignment and other irregularities. Power in the HOMs is not available for heating.

Transmission lines use straight pieces connected by miterbends, which are boxes with a mirror. Inside the box, the waveguide walls are effectively missing, which leads to diffraction losses. These take the form of reflections and HOMs.

To quantify the losses and compare with existing methods, a 90° miterbend is simulated with the fullwave code IPF-FD3D. Fig. 1 shows the HOM fields in the miterbend, where the beam enters from the bottom and exits to the right. The loss is less than 1%.

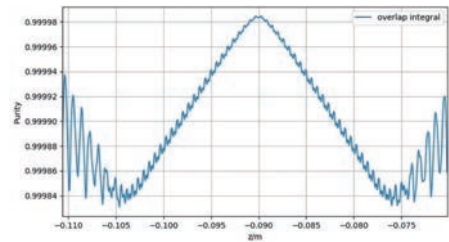


Fig. 2: Mode purity of the fundamental mode in the input waveguide along the waveguide axis.

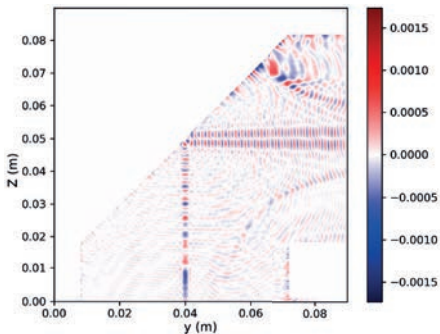


Fig. 1: Electric field of the higher order modes generated by the miterbend in the y-z plane.

Fig. 2 shows the mode purity of the simulated input field along the axis of the input waveguide, which should be 100% fundamental. Only 0.0016% of the power are not in the fundamental mode, giving a very high accuracy for calculating the loss.

Funding: University of Electronic Science and Technology of China, School of Electronic Science and Engineering, Chengdu, China



Comb reflectometer backend for fusion plasmas

Walter Kasperek

Conventional reflectometers only send and receive a single frequency at the time. Several simultaneously launched frequencies of a Doppler reflectometer could obtain, in a single measurement, the radial distribution of the fluctuation spectrum or, with a frequency-scanned antenna, the wavenumber spectrum of the fluctuations at a fixed radius. For applications at ASDEX Upgrade, the transmitter-receiver electronics of such a comb-reflectometer for millimeter waves in the W-Band (75–110 GHz) have been developed and built.

stages with four mixers, which convert the W-Band signal to three final IF frequencies in the 900 MHz range. The third stage with 7 narrowband filters and subsequent IQ-mixers provides both amplitude and phase, and thus the propagation direction of the plasma fluctuations.

The hardware is contained in three 19-inch chassis, which have been delivered to ASDEX Upgrade for the installation of the power supplies.

A first operation of the hardware was successfully demonstrated in experiments in June 2021 at ASDEX Upgrade.

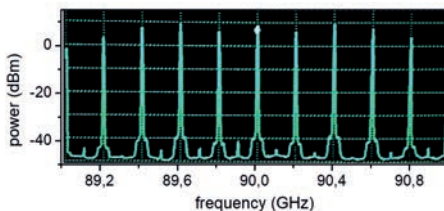


Fig. 1: Typical comb spectrum, generated by 200 MHz DSB modulation of a 15 GHz source and a subsequent hexupler.

The generation of the frequency comb (7 frequencies in the W-Band, comb frequency step-adjustable from 0.11 GHz to 6 GHz) is done in a multiplier (hexupler) driven by 3 frequencies from two synthesizers and double-sideband mixing. An example is shown in Fig. 1. A W-Band amplifier is used at the output to the plasma. The heterodyne receiver for the plasma reflections consists of 2 mixing

Publication: Happel, T., Kasperek, W., Hennequin, P., Höfler, K., Honoré, C. and the ASDEX Upgrade Team (2020) Design of a variable frequency comb reflectometer system for the ASDEX Upgrade tokamak, *Plasma Sci. Technol.* 22 064002, <https://doi.org/10.1088/2058-6272/ab618c>

Collaboration: Tim Happel and Klara Höfler, Max Planck Institute for Plasma Physics (IPP), Garching; Pascale Hennequin and Cyrille Honoré, Laboratoire de Physique des Plasmas (LPP), Palaiseau, France

Funding: Max Planck Institute for Plasma Physics (IPP), Garching and Greifswald

Plasma dynamical processes in generation and confinement

Mirko Ramisch, Alf Köhn-Seemann



Nuclear fusion provides an energy source with zero carbon emission and an efficiency 6 orders of magnitude above burning fossil fuels. Fusion energy – when established – will ensure a supply as compliant with the UN Sustainable Development Goals on the long term. In this frame, the Plasma Dynamics and Diagnostics group at IGVP contributes to fundamental research and education in particular as part of a knowledge-sharing international consortium.

Key issues of fusion research are to find conditions under which hot (beyond 10 million Kelvin) and dense fusion plasmas can be sustained and confined for a sufficiently long time as to achieve a positive net energy outcome from fusion reactions for utilization in future power plants. Conceptually, these plasmas are confined in toroidal magnetic field configurations allowing for central peak energy densities. Steep density gradients in the plasma edge region, however, can prevent electromagnetic waves from reaching absorption layers for efficient heating. Moreover, plasma fluctuations arising from these gradients can cause turbulent cross-field transport of particles and heat out of the confinement region and, thus, affect thermal isolation of the plasma.

At the IGVP, the stellarator experiment TJ-K is operated with low-temperature plasmas for the purpose of conducting fundamental research in the fields of plasma/microwave interactions and plasma turbulence. To capture the non-linear spatio-temporal plasma dynamics, specifically developed diagnostics, e.g. probe arrays, are employed. Studies on wave-conversion processes aim at a detailed understanding of efficient heating scenarios incorporating wave scattering processes at turbulence-distorted boundary layers. The microscopic turbulent dynamics across the interface between confined plasma and scrape-off layer determines the global confinement. The mechanisms of self-generated flows and flow/turbulence interactions are studied in dependence on the magnetic field geometry in view of possible transport control or optimization options.

Experimental investigations are supported by complementary simulations using high-level codes developed on-site or at the Max Planck Institute for Plasma Physics (IPP).

Funding: ErasmusMundus Master program “European Master of Science in Nuclear Fusion and Engineering Physics”; German Research Foundation (DFG); Max Planck Institute for Plasma Physics (IPP), Garching and Greifswald



Numerical feasibility study of electron Bernstein wave heating in LTX- β

Alf Köhn-Seemann

The plasma-facing inner wall components of large-scale fusion experiments need to withstand high heat fluxes of up to 20 MW/m². Tungsten is currently used in most devices, showing promising results in experiments across the world. A challenge is the regular need for replacement requiring shut-down times which are in particular problematic for a potential fusion power plant. Liquid surfaces, where the plasma-facing inner wall surface is constantly renewed, are considered as an alternative solution. LTX- β is a small-scale tokamak dedicated to study liquid lithium as a first-wall material.

LTX- β is routinely operated with over-dense plasmas, where the electron plasma frequency exceeds the electron cyclotron frequency. Transferring microwave energy to the plasma thus requires operating the microwave heating system at harmonics of the cyclotron frequency which is only efficient for high electron temperatures. Here we explore an alternative approach where the injected microwave couples to the electrostatic electron Bernstein wave (EBW). Full-wave simulations are performed in order to identify the optimum coupling efficiency.

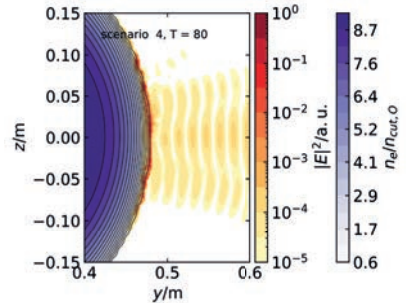


Fig. 1: Snapshot of the absolute value of the squared wave electric field as obtained from full-wave simulations.

Two scenarios are possible to couple to the EBW: One favors more shallow density gradients, whereas the other favors steep profiles. Both mechanisms could be successfully identified in the simulations, each featuring a different parameter range. Fig. 1 shows as an example a full-wave simulations, where a coupling efficiency of 75 % has been achieved. The enhancement of the wave electric field in the coupling region can clearly be seen.

Publication: Anderson, J. K., Diem, S., Köhn-Seemann, A. (2020) Numerical simulations for evaluation of EBW Heating development in LTX- β , 62nd Annual Meeting of the APS Division of Plasma Physics, http://absimage.aps.org/image/DPP20/MWS_DPP20-2020-001786.pdf

Collaboration: B. M. Kenia, University of Wisconsin-Madison, Wisconsin; J. K. Anderson, University of Wisconsin-Madison, Wisconsin

Funding: Max Planck Institute for Plasma Physics (IPP), Garching and Greifswald



Simulation of the O-SX-B mode conversion process in the TJ-K stellarator

Eberhard Holzhauer, Alf Köhn-Seemann

The electrostatic electron Bernstein wave (EBW) provides a method to transfer energy to over-dense plasmas where the electron plasma frequency is above the electron cyclotron frequency making them inaccessible for conventional microwave heating scenarios. Due to their electrostatic nature, the EBW needs to be coupled to externally injected microwaves. One of these coupling scenarios is the O-SX-B conversion: a microwave in O-mode polarization is injected into the plasma under an optimal angle with respect to the background magnetic field. At the O-mode cut-off, the wave couples to an SX-mode which is reflected at the so-called turning point and starts to propagate outwards again. In the vicinity of the upper-hybrid resonance, the SX-mode couples to the backwards propagating EBW.

The O-SX-B coupling scenario has been successfully realized at the TJ-K stellarator with an 8 GHz microwave heating system. In parallel with the experiments, we have started to perform ray-tracing calculations, as shown in Fig. 1. One can clearly identify the locations where the different coupling processes take place. The EBW turns into the toroidal direction inside of the plasma and asymptotically approaches the electron cyclotron resonance.

Funding: Max Planck Institute for Plasma Physics (IPP), Garching and Greifswald

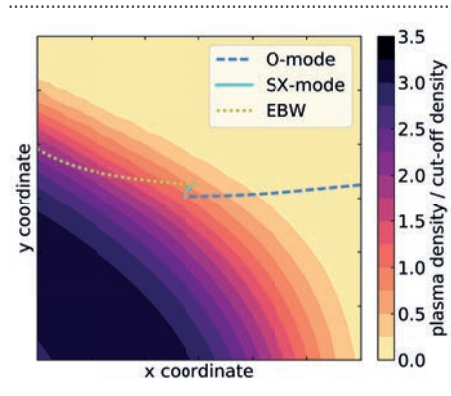


Fig. 1: Ray-tracing simulations of the O-SX-B coupling scenario for the 8 GHz heating system in the TJ-K stellarator. The different branches of the microwave are labeled in the plot. Color-coded is the electron plasma density normalized to the O-mode cut-off density.



Plasma electrons' acceleration up to energies of 100 keV

Alf Köhn-Seemann

Microwave heating of over-dense plasmas is routinely achieved in the stellarator TJ-K. In contrast to usually applied heating scenarios at tokamaks or stellarators, we found an operational regime in TJ-K where the heating occurs well below the electron cyclotron frequency. After coupling of the injected microwave to Whistler-waves in the plasma, microwave energy is deposited in the vicinity of the so-called O-resonance. The accompanying large wave electric fields are thought to be responsible for a small population of high-energy electrons.

A soft X-ray diagnostics, provided by the IPP Greifswald, allowed for the first time to quantify the energy of the fast electrons. The diagnostics consists of the semi-conductor detector, a Si(Li) diode in reversed biased configuration, sensitive to soft X-rays emitted by the high-energy electrons during their interaction with the plasma ions. A pulse height analyzer together with a calibration unit is then used to obtain an energy spectrum up to a detection limit of 200 keV.

A spectrum obtained by the diagnostics is shown in the figure. The characteristic lines are due to the interaction of the fast electrons with the vacuum vessel. The soft X-ray radiation emitted by the fast electrons exhibits an exponential dependence on their temperature. A

linear fit to the semi-logarithmic plot allows thus to determine the temperature. We were able to detect maximum values of up to 100 keV in this operational scenario, with the bulk electrons being at significant lower temperature of approximately 10 eV. The detected high energies are in-line with a model describing the acceleration of electrons in the wave electric field.

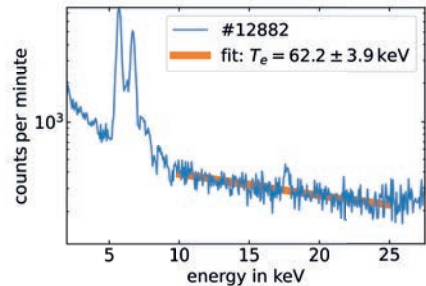


Fig. 1: Soft X-ray spectrum of high-energy electrons in TJ-K, obtained from the pulse height analyzer. The characteristic lines originate from interactions of the electrons with the stainless steel vacuum vessel of TJ-K. The linear fit to the continuous part of the spectrum is used to determine the temperature of the fast electrons.

Publication: Köhn-Seemann, A., Birkenmeier, G., Diez, P., Holzhauser, E., Merli, S., Ramisch, M., Sichardt, G., Stroth, U. (2022) Plasma electron acceleration in a non-resonant microwave heating scheme below the electron cyclotron frequency, *New J. Phys.*, 24 No. 063024, <https://doi.org/10.1088/1367-2630/ac747a>

Collaboration: U. Stroth, Max Planck Institute for Plasma Physics (IPP), Garching

Funding: Max Planck Institute for Plasma Physics (IPP), Garching and Greifswald



Influence of plasma density fluctuations on wave coupling scenarios

Alf Köhn-Seemann

Coupling externally injected microwaves to plasmas where the plasma density exceeds the cut-off density can be achieved via electron Bernstein waves (EBWs). These are electrostatic waves that can propagate in arbitrarily high-density plasmas and are very well absorbed at the electron cyclotron resonance and its harmonics, even at low electron temperatures. Furthermore, EBWs can drive very efficiently currents in plasmas, which is of particular importance in tokamaks to increase their discharge time towards a steady state device.

EBWs can be excited via a two-step mode coupling process: an injected O-mode couples to an X-mode at the O-mode cut-off layer and then propagates outwards towards the upper-hybrid resonance where it couples to the backwards propagating EBW. The overall efficiency of this coupling process is strongly dominated by the O-X conversion which itself depends on injecting the microwaves at a correct angle with respect to the background magnetic field. Plasma density fluctuations in-front of the conversion layer, leading to a deflection of the microwave beam, can therefore perturb the conversion process and thus reduce the overall heating efficiency.

We have performed full-wave simulations of the O-X coupling process taking into account the effect of turbulent

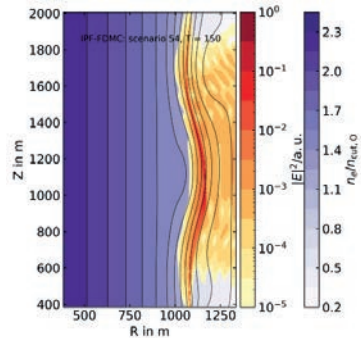


Fig. 1: Electron plasma density and a snapshot of the squared wave electric field as obtained from full-wave simulations for one sample.

plasma density fluctuations. A synthetic turbulence generator has been used to generate an ensemble of profiles fed into the simulations. Fig. 1 shows as an example the case for one sample drawn from a full ensemble: the microwave is injected from the right and enhancement at the plasma boundary can be clearly seen. This is where the coupling takes place and where the X-mode is, in these simulations, damped at the upper-hybrid resonance. The perturbation of the conversion layer results in this case in a reduction of the conversion process on the order of 20%.

Collaboration: L. A. Holland, R. G.L. Vann, York Plasma Institute, U.K.; B. Eliasson, D. Woodward, University of Strathclyde, Glasgow, U.K.; S. J. Freethy, Culham Centre for Fusion Energy, U.K.

Funding: Max Planck Institute for Plasma Physics (IPP), Garching and Greifswald



FDTD full-wave simulations and interferometry measurements for microwave-plasma interactions

Christos Vagkidis, Alf Köhn-Seemann, Günter Tovar

Interferometry is widely used in plasma physics to obtain the line-integrated density of a plasma. A novel interferometry approach is developed to estimate the plasma density profile, apart from the line-integrated density, with accompanying full-wave simulations. A stable microwave-generated plasma torch is used, which is confined in a glass quartz tube. The interferometer is realised using a network analyzer and a high frequency microwave beam is used as probing ray. It is emitted by a horn antenna and crosses the cylindrical-shaped plasma perpendicularly to the cylindrical axis. The receiving antenna is placed on the other side of the plasma and is aligned with the sending antenna. Despite the beam scattering, the phase difference can still be measured by the receiving antenna and is used to calculate the line-integrated density. The spatial distribution of the probing beam is obtained by moving the receiving antenna.

One of the most robust methods to describe electromagnetic wave propagation, such as microwave propagation, is the full-wave solution, since Maxwell's equations are exactly solved. Based on Yee's algorithm, a 2D Finite-Difference Time-Domain (FDTD) full-wave code is being developed. The electric and magnetic fields (E , B) of the microwave beam are evolved with the leapfrog method in both time and space. The

plasma current density (J) from the linearised fluid equation is also evolved and accounts for plasma effects. Essentially, this leads to an explicit calculation of E , B and J for each time step. The beam is propagating across a quartz tube and a circular plasma. The spatial profile of the beam power is monitored in the receiving antenna plane, and it is shown how the shape depends on the plasma density profile. Finally, by comparing simulation and experimental results, the actual plasma shape can be deduced. Fig. 1 illustrates a good comparison between the measured experimental beam power against the calculated power from the simulation.

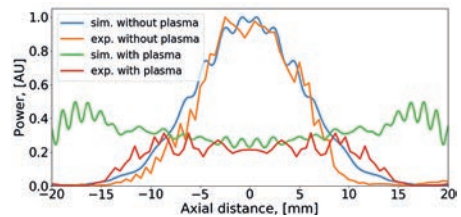


Fig. 1: Comparison of scattered-wave power distribution between simulation and experiment. The center of the plasma is assumed to be at $z = 0$ mm and the plasma density is normalised to the cut-off density.

Funding: Max Planck Institute for Plasma Physics (IPP), Garching and Greifswald



Tilt angle analysis of turbulent structures with the ellipsoidal model

Til Ullmann, Mirko Ramisch,
Bernhard Schmid, Günter Tovar

In magnetized fusion plasmas, radially varying tilt angles of turbulent structures lead to the formation of zonal flows (ZF) that can trigger the high-confinement mode. Formally, ZF formation is expressed in terms of the radial gradient in the Reynolds Stress (RS), which can be calculated as averaged product of radial and poloidal velocity fluctuations. For the interpretation of the RS as measure of turbulent vortex tilt, the RS is to be compared with the actual tilt of the structures, which can be calculated using the ellipsoidal model.

For this purpose, potential fluctuations are measured at the stellarator TJ-K using an array of 128 flux-surface aligned Langmuir probes with radial and poloidal as well as a high temporal resolution. From the data the ExB velocity fluctuations can be obtained, from which the time-averaged RS for differ-

ent positions is calculated. In addition, cross correlation functions (CCF) of fluctuations at individual measuring positions are used to determine the shape of coherent structures. The CCFs with respect to a reference position for two spatial shifts (ϵ_1, ϵ_2) and a time lag (τ) are shown in Fig. 1. From the figure, the ellipsoidal character of the CCFs can be seen. For fixed $\tau=0$, the CCFs reduce to an ellipse as described by $0 = \epsilon_1^2/\rho_1^2 + (\epsilon_2 - a\epsilon_1)^2/\rho_2^2$. The factor a reflects the tilt angle of the turbulent structure and can be calculated by regression. As shown in Fig. 2 the tilt correlates with the RS, which confirms the RS as a measure for the tilt of turbulent structures.

Collaboration: P. Manz, Institute of Physics, University of Greifswald

Funding: Max Planck Institute for Plasma Physics (IPP), Garching and Greifswald

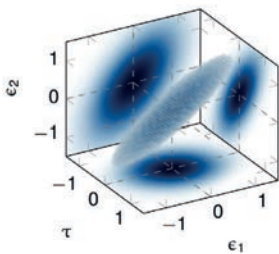


Fig. 1: The shown ellipsoid models the cross-correlation function around its maximum in the radial and poloidal space as well as time domain.

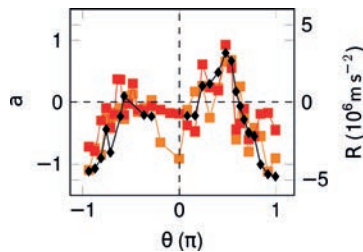


Fig. 2: Comparison of the tilt (a) of turbulent vortices and the RS (square) on two consecutive flux surfaces. Tilt and RS show a qualitatively good agreement.



Enhancement of energy transfer to zonal flows by stationary shear flows

Til Ullmann, Mirko Ramisch, Bernhard Schmid, Günter Tovar

Turbulence-driven zonal flows (ZFs) can trigger the high confinement mode in fusion plasmas. In this process, stationary shear flows can influence the energy transfer between zonal flows and turbulence. In the frame of the $k-\varepsilon$ model, this transfer is quantified by the dedicated production term: It is determined as product of Reynolds stress (RS), measuring the correlation of radial and poloidal velocity components, and the background flow shear. In this model, the nonlinear RS can be approximated linearly by the flow shear, resulting in a quadratic dependence of the energy transfer on the shearing rate. Hence, with increasing shearing rate, one would expect an enhanced redistribution of turbulent power in favor of large-scale ZFs.

At the stellarator TJ-K, the zonal RS distribution is measured with Langmuir-probe arrays. The stationary background shear flow is obtained from potential measurement, under variation through external plasma biasing. Fig. 1 (top) shows the linear dependence of the RS on the shearing rate and Fig. 1 (middle) the quadratic dependence of the production term, both consistent with theory. Fig. 1 (bottom) shows the relative ZF power. It increases parabolically over the full shear range, demonstrating enhanced ZF drive through stationary shear flows.

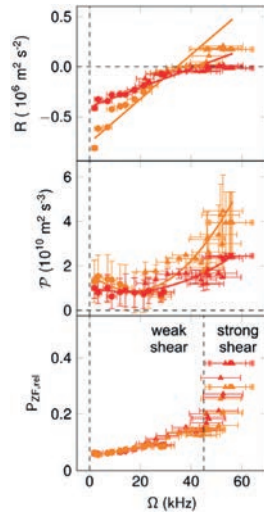


Fig. 1: Behavior of the zonally and temporally averaged RS (top) for two flux surfaces (orange, inner and red, outer), the production term (middle), and relative ZF power (bottom) with background ExB shearing rate. Positive production indicates energy transfer from turbulence into the ZF.

Publications: Ullmann, T., Schmid, B., Manz, P., van Milligen, B., Tovar, G. E. M., Ramisch, M. (2020) Experimental observation of resonance manifold shrinking under zonal flow shear, *Phys. Rev. E*, 102 No. 063201, <https://doi.org/10.1103/PhysRevE.102.063201>
Ullmann, T., Schmid, B., Manz, P., Tovar, G. E. M., Ramisch, M. (2021) Turbulent energy transfer into zonal flows from the weak to the strong flow shear regime in the stellarator TJ-K, *Phys. Plasmas*, 28 No. 052502, <https://doi.org/10.1063/5.0039959>

Collaboration: P. Manz, Institute of Physics, University of Greifswald

Funding: Max Planck Institute for Plasma Physics (IPP), Garching and Greifswald



Interplay of turbulent density and momentum transport in TJ-K plasmas

Ralph Sarkis, Mirko Ramisch,
Bernhard Schmid, Günter Tovar

As a result of prior findings, a study has been initiated on the interplay between turbulent particle transport and momentum transport, better known as Reynolds stress, in magnetized plasmas. Turbulent plasma dynamics is highly influenced by the geometry, which is moulded by the magnetic field. At the TJ-K stellarator, it was observed that the plasma confining magnetic field gives rise to localized enhancement of intermittency and turbulent transport, as a result of localized decoupling through curvature effects. The Reynolds stress, recognized as transport of momentum, is a measure of vortex tilt. Therefore, Reynolds stress denotes a deformation in the shape of turbulent structures. For magnetized plasmas, strong density potential cross-coupling promotes high levels of Reynolds stress. Whilst, it was also noticed at TJ-K, that the Reynolds stress peaks in the region with maximum particle transport and intermittency levels.

The coincidence of both transport phenomena is contrarian to expectations as the Reynolds stress is favoured by coupling, while turbulent transport is a result of decoupling, which are both mutually exclusive prerequisites. The aim is to establish a detailed understanding of turbulent transport phenomena in dependence of the geometry, and to examine temporal alternations in the density-potential cross-coupling as

a possible explanation for their coexistence. A special challenge is to resolve both types of transport poloidally at the same time for correlation analyses. In a first step, conditional sampling of transport with respect to the occurrence of zonal-potential events may be utilized to address this issue. More advanced studies shall address the interplay of both transport types on a spectral level in order to distinguish amplitude from phase modulations.

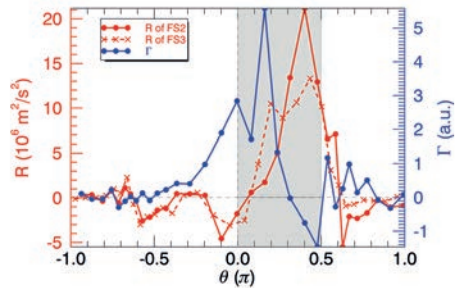


Fig. 1: Poloidal profile of the Reynolds stress R (red) on two neighbouring flux surfaces, and that of the cross-field particle transport Γ (blue). It is observed that both turbulent transport phenomena peak in the region with negative normal curvature and positive geodesic curvature.

Funding: Funded by the Deutsche Forschungsgemeinschaft (DFG, German Research Foundation) – 471314753



Causality analysis of the drift-wave – zonal flow system at the stellarator TJ-K

Nicolas Dumérat, Mirko Ramisch, Bernhard Schmid, Günter Tovar

The use of Convergent Cross Mapping (CCM) as a causality inference technique has proven its capacity for unveiling causal coupling between two variables measured in the same dynamical system. CCM describes a measure of how well the mapping – from a small region within a multidimensional phase space reconstruction in one variable (from time-delay embedding) – compares to the actual representatives of the second variable in its reconstructed phase space. A divergent behaviour resulting from the lack of a causal relationship would be reflected in small measures.

In our case, the CCM is applied to Langmuir probe measurements from the stellarator TJ-K. The drift-wave – zonal flow interaction is of crucial interest to understand turbulence in magnetic fusion devices. Indeed, it is known that the presence of stable shear flows tends to suppress turbulence. This two-species system is often referred to as a Predator and Prey system. The frequency scale separation existing in TJ-K turbulent structures allows for the separation of each component, letting us analyze them individually.

Through the use of digital bandpass filters and averaging techniques, the causal dependencies between time scales in measurements can be established. As shown in the picture, for longer time series, the prediction skills converge but don't reach the same values depending on the direction. According to the CCM results, a clear causal dependence between the 10–40 kHz range, and the 0–10kHz range is established. This could be a sign of the inverse turbulent cascade, validating the hypothesis that the background turbulence causes the growth of the zonal flows.

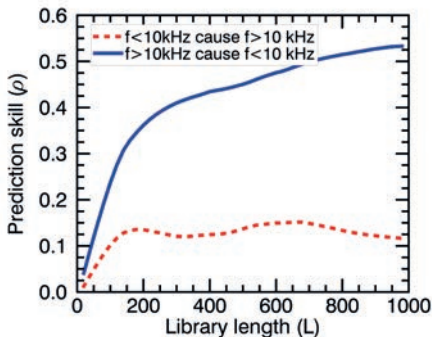


Fig. 1: Convergent cross-mapping for potential fluctuations taken for two distinct frequency bandwidths. Both directions converge for increasing data length and the prediction increases significantly for one specific direction indicating an unidirectional coupling.

Funding: Max Planck Institute for Plasma Physics (IPP), Garching and Greifswald



Collisionality dependence of spectral power distribution

Yu Chun Lin, Mirko Ramisch

In the Hasegawa-Wakatani turbulence model, the collisionality controls the parallel response of electrons to plasma perturbations elongated along to the magnetic field lines. An adiabatic, i.e. instantaneous, response at low collisionality results in an in-phase coupling of density with potential perturbations, whereas density perturbations affect the plasma flow. With increasing collisionality the system develops into the hydrodynamic limit, where density and potential decouple. Here, the density evolves rather like the vorticity as it is just advected passively in the flow field. Theoretically, the transition from the adiabatic to the hydrodynamic limit should be accompanied by a change in the turbulence characteristics, in particular in the typical time scales, from long to short auto-correlation times. Correspondingly, a change in spectral characteristics is expected from a narrower to a broader power distribution in the frequency power spectra.

At TJ-K, the plasma discharge conditions can be varied via the working gas to cover the collisionality regimes from adiabatic to hydrodynamic. This flexibility provides an ideal test bed for proving theoretical expectations for the spectral width of turbulent power distribution at the transition between these regimes. Fig.1 shows an example of frequency power spectra of density fluctuations within the wavenumber

range $1 < k\rho_s < 2$ as measured for gases H, He and Ar with a poloidal probe array. As the collisionality drops with increasing ion mass (m_i), the observed trend of increasing spectral width with increasing collisionality complies with expectations from Hasegawa-Wakatani simulations.

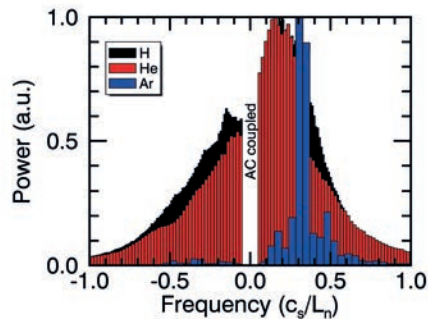


Fig. 1: Frequency power spectra of plasma density perturbations propagating in the electron diamagnetic drift direction. The spectral width increases with collisionality ($\sim m_i^{-1}$).

Collaboration: P. Manz, Institute of Physics, University of Greifswald

Funding: ErasmusMundus Master program "European Master of Science in Nuclear Fusion and Engineering Physics"



Turbulence classification using artificial neural networks

Mirko Ramisch

Convolutional neural networks (CNN) have proven applicable for pattern recognition in various areas, e.g. in processing audio signals or image data. Based on intrinsic features, they can be trained to distinguish objects within a given set of categories. To this end, basically convolution kernels are optimized to detect these features, which are not predefined but rather crystallize as characteristic for the specific categories during training.

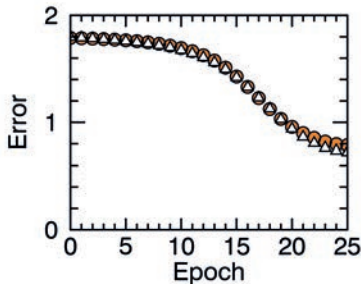


Fig. 1: Log-likelihood curves for working gas classification of turbulent density fluctuations, with the CNN trained on 192 subseries per epoch (triangles) and accordingly tested on independent generalizations (circles).

This is an interesting aspect in analyzing turbulence time series, which hold coherent contributions. Limitations through ambient turbulence are reflected in typical correlation times and lengths. Moreover, the microscopic characteristics of turbulent fluctuations in magnetized plasmas show a collision-

ality dependence, for which its ion-mass dependence can be exploited in experimental scaling studies. For such a purpose, the working-gas at the stellarator experiment TJ-K can be flexibly chosen from H, D, He, Ne, Ar and Kr. Hence, as each gas comes along with its specific turbulence characteristics, CNNs may be tested for their capability to determine the gas type on the basis of “hidden” dynamical features.

First attempts with a CNN, consisting of two correlation/pooling stages with leaky rectified linear units, were carried out on time series of turbulent density fluctuations. The stages use 48 and 1 kernels of size 128 per input, respectively. Input dimensions are sequentially reduced from 1024 to 256 before flattening. This is followed by the final softmax categorization into 6 classes, i.e. gas types. The corresponding error curves in Fig. 1 demonstrate that the network improves in predicting the gases from independent turbulent time series as generalization during training. Despite the promising trend, detection reliability remains to be improved. In further studies, this network type may prove useful as tool for analyzing turbulent fluctuations with special regard to structural analysis and precursor detection.

Funding: Max Planck Institute for Plasma Physics (IPP), Garching and Greifswald

Investigation into the spatial distribution of intermittency at the stellarator TJ-K

Henrik Beeck, Mirko Ramisch



Intermittency in plasma fluctuations can lead to a significant fraction of high-amplitude transport events, which are potentially harmful to the periphery at the edge of magnetically confined fusion plasmas. Therefore, it is important to get a better understanding of how intermittency is generated in such systems. To this end, intermittency in plasma density fluctuations are resolved in the entire poloidal cross section of the stellarator experiment TJ-K and compared to geometrical properties of the confining magnetic field or characteristics of plasma flows.

Previous investigations already indicated a dependence of intermittency on curvature and adiabaticity. With a poloidal probe array, a rough spatial coincidence of higher intermittency levels with the curvature driven destabilization of drift waves was found. Consistently, lower adiabaticity was found to be accompanied by stronger intermittency. In the present work, a broader spatial coverage is achieved. In a first step, structure functions are analyzed for deviations (μ) from self-similarity, that is opposed to local destabilization of drift waves. Measurements with different gases confirm previously observed trends with the adiabaticity, i.e. more intermittency in lighter gases. For a hydrogen discharge, the levels μ are compared to local curvature drive in Fig. 1. If projected onto a flux surface in

the density gradient region, previous results are roughly reproduced. However, a more complex poloidal and radial pattern becomes visible.

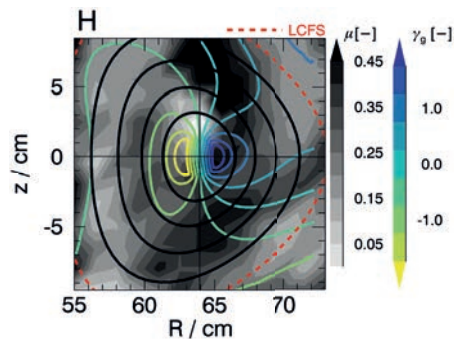


Fig. 1: Contour plot of density intermittency levels in the poloidal cross section. The colored contour lines depict local maximum linear growth rates of drift-wave turbulence. Growth rates and intermittency levels show a similar up-down asymmetry.

In a next step, the role of magnetic and flow shear will be examined, the latter in particular by means of the so-called Okubo-Weiss parameter, which predicts the regions with exponential growth of passively advected scalars.

Collaboration: G. Herdrich, Institute of Space Systems, University of Stuttgart



Non-locality of particle transport in the stellarator TJ-K

Nils Müller, Mirko Ramisch

Turbulent transport perpendicular to the magnetic field significantly deteriorates the quality of magnetically confined plasmas. In particular, current transport modeling predominantly follows a diffusive paradigm, but there are non-diffusive theories, which incorporate non-local plasma interactions. The extent and characteristics of non-local transport contributions were investigated experimentally in TJ-K. A non-diffusive, convolution-based method is applied. The kernel function K_r allows an arbitrary relationship between transport Γ and the density gradient ∇n : $\Gamma(r) = -\int K_r(r-r') \nabla n(r') dr'$.

This model resolves non-local, turbulent transport in TJ-K via Fourier transformed kernel functions $F(K_r)$, where diffusive transport would show up as $F(K_r)(k_r) = \text{const}$. Observed functions, however, depend on the wave number. Fig. 1 shows these kernels in terms of the normalized wave number k_r for helium discharges.

Three regimes persist across all working gases and pressures. The maximum gradient decay length L_n is proposed as an upper bound for the non-diffusive structures in the system, which could explain the plateau regime in the kernels at low wave numbers. At intermediate scales, the kernel is consistent with super-diffusive transport processes. At smaller scales, the shape might be attributed to sub-diffusion as associated with particle trapping in small vortices or on scales of the ion Larmor radius. The typical interaction distances in those regimes exhibit a distinct dependency on characteristic wave numbers, while a pressure dependence remains unclear.

Collaboration: P. Manz, Institute of Physics, University of Greifswald; M. Brüggen, Hamburg Observatory, University of Hamburg

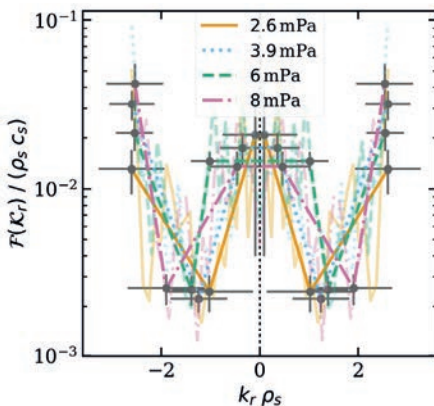


Fig. 1: Fourier transformed kernels $|F(K_r)|$ with piece-wise linear fits. Axes are normalized by the drift scale ρ_s and ion sound speed c_s .



Turbulence transport across magnetic islands

Mirko Ramisch

Magnetic islands are intrinsic to toroidal plasma confining magnetic fields, e.g. wherever current filaments are introduced by MHD instabilities or parasitic error fields perturb the magnetic field structure. They could affect the quality of confinement either way: degrading confinement by enhancing cross-field transport or even improving confinement by developing encapsulated equilibria in which shear-flow generation reduce turbulence.

In order to investigate the impact of magnetic islands on the transport of turbulence, i.e. via turbulent transport or turbulence spreading, TJ-K's flexibility in shaping the magnetic field is employed. To this end the ratio of the current through the helical and compensating vertical field coils of the torsatron type configuration allows to shift the magnetic axis radially, whilst the radial profile of the rotational transform passes regions of different low-order rationals, where islands are generated.

For helium discharges in two exemplary island configurations, Fig. 1 shows the turbulence driving rate $\partial_t \ln P = \omega_D + \omega_S$ – with $P = \langle \tilde{n}^2 \rangle / 2$ the power in the density fluctuations, $\omega_D = -\partial_r n \langle \tilde{v}_r \tilde{n} \rangle / P$ the local driving rate, and $\omega_S = -\partial_r \langle \tilde{v}_r \tilde{n}^2 \rangle / (2P)$ the turbulence spreading rate – in comparison to the standard configuration without islands (current ratio $R_{vh} = 57\%$). For $R_{vh} = 58.6\%$, iota passes 1/5 near the

separatrix resulting in a narrow $m = 5$ island chain, which is passed by the movable Langmuir probe close to an X-point. For $R_{vh} = 53\%$, an $m = 3$ island chain with increased radial width is obtained. While through the X-point the driving-rate profiles do not strongly differ from the island-less configuration, the O-point setup shows slightly reduced transport. More detailed studies are ongoing.

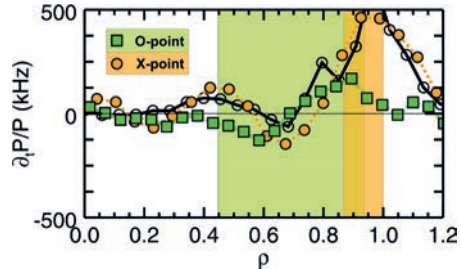
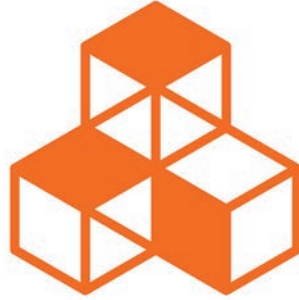


Fig. 1: Profiles of the driving rate in density fluctuations with islands (●: across O-point; ■: close to X-point) and without islands (○, solid) against normalized radius. The island widths are indicated by shaded areas. Reduced transport is observed across the O-point.

Collaboration: P. Manz, Institute of Physics, University of Greifswald

Funding: Max Planck Institute for Plasma Physics (IPP), Garching and Greifswald

9 INDUSTRY, INNOVATION AND INFRASTRUCTURE



Emission spectroscopic and high-speed camera measurements at water vapor arc plasma

Andreas Schulz, Stefan Merli, Matthias Walker



The disposal and reuse of plastics has become the focus of public attention worldwide. Various technologies for the pyrolysis of plastic waste are currently under investigation (“waste-to-energy”). In order to be able to use the resulting gas as synthesis gas (“syn-gas”), e.g. to generate energy, further processing steps are necessary. Several studies have shown that water steam plasma represents a promising technical solution. However, the typical power range of 20 kW of such plasma sources is not sufficient. Plasma sources up to 100 kW must be developed and investigated for large-scale applications. In order to be able to use the process in a targeted manner, it is necessary to determine the physical and chemical parameters of the plasma flame. For this purpose, emission spectroscopic studies and high-speed camera diagnostics were carried out.



Fig. 1: Image of the plasma torch.



Fig. 2: Image of the water damp arc plasma with afterglow.

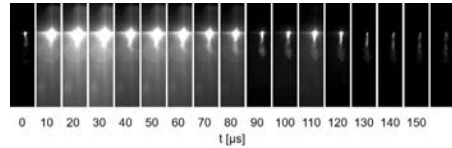


Fig. 3: Image of a typical plasma ejection sequence from the nozzle opening. The quasi-pulse is typically 150 μ s. In the last picture the next plasma ejection sequence starts.

In order for a water damp plasma to be examined spectroscopically, the temporal behavior must be considered. The recordings of the plasma with a high-speed camera show a quasi-pulsed behavior. Fig. 3 shows a typical plasma ejection sequence from the nozzle opening. The quasi-pulse is typically 150 μ s. In the last picture the next plasma ejection sequence starts. Different areas had to be considered for the evaluation of the spectroscopic data: At the nozzle exit the hydrogen lines of the hydrogen Balmer series can be observed in the bright emission area. The excitation temperature of the electrons could be obtained from the evaluation of the Maxwell Boltzmann distribution Balmer emission lines directly at the nozzle opening. Fig. 4 shows the Boltzmann plot. The evaluation using a regression line results in an excitation temperature of $T_{\text{ex}} = (4180 \pm 350)$ K. Almost no emission of the OH radical can be determined at the nozzle exit. From this it is concluded that the water in the plasma torch is completely dissociated. Just

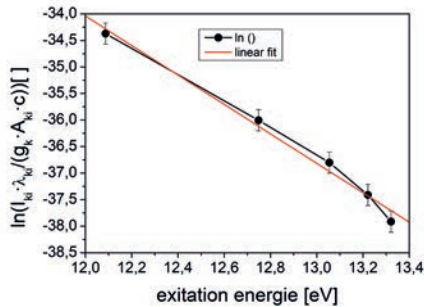


Fig. 4: Image shows the Boltzmann plot of the hydrogen Balmer series. The evaluation using a regression line results in an excitation temperature of $T_{\text{ex}} = (4180 \pm 350)$ K.

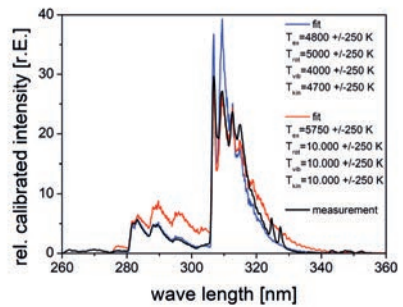


Fig. 5: Image of the OH rotation-vibration band in the spectral range from 280 nm to 330 nm. Two temperatures can be determined from the band shape: $T_{\text{rot}} = T_{\text{vib}} = (10.000 \pm 250)$ K for the plasma ejection in the quasi-pulse and $T_{\text{rot}} \approx T_{\text{vib}} \approx (4500 \pm 500)$ K for the afterglow.

two centimeters after the nozzle, the OH rotation-vibration band dominates in the spectral range from 280 nm to 330 nm. Two temperatures can be determined from the band shape: $T_{\text{rot}} = T_{\text{vib}} = T_{\text{kin}} = (10.000 \pm 250)$ K for the plasma ejection in the quasi-pulse and $T_{\text{rot}} \approx T_{\text{vib}} \approx T_{\text{kin}} \approx (4500 \pm 500)$ K for the afterglow. For the project, the spatial and temporal distributions of the temperatures were determined and the dynamics of the quasi-pulsed operation were studied. From these findings, optimal operating parameters for synthesis gas production could be derived.

Collaboration: PlasmaAir AG, Weil der Stadt

Funding: German Federal Ministry for Economic Affairs and Energy (BMWi), Zentrales Innovationsprogramm Mittelstand FKZ.: ZF4414603DF9

Optical emission spectroscopy of a CO₂/H₂ microwave plasma

Marc Bresser, Andreas Schulz, Matthias Walker, Günter Tovar

The chemical industry is largely dependent on fossil fuels for the production of organic substances and needs to find a renewable way to produce carbon-based molecules. Methanol is considered one of the most important basic chemicals. One possible new way to produce methanol is to use an atmospheric pressure microwave plasma torch with carbon dioxide (CO₂) and “green” hydrogen. The CO₂ plasma produces carbon monoxide (CO) and oxygen. The added hydrogen is used to react with the CO and produce methanol. The methanol is separated from the other gases (CO, O₂ and CO₂) after the plasma torch by condensation with a water-cooling. If renewable energy is used for the plasma generation, the entire process of methanol production is sustainable. Optical emission spectroscopy (OES) in the range of UV to IR is used to characterize the plasma. In the CO₂ plasma the C2-Swan bands dominate the spectrum. The C I and O I lines can also be seen in the spectrum. When hydrogen is added to the plasma, the three additional active species OH, CH and H I are found.

Collaboration: Technische Universität Darmstadt (TU Darmstadt), Darmstadt; Fraunhofer Institut for Engineering and Biotechnology (IGB), Stuttgart; Plasus GmbH, Mering; Muegge GmbH, Reichelsheim; Evonik Operations GmbH, Essen; Resources + Technologies-Management (RTM), Bornheim

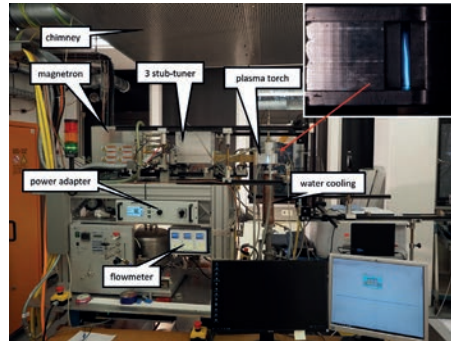


Fig. 1: Image of the NexPlas lab and a CO₂ plasma torch.

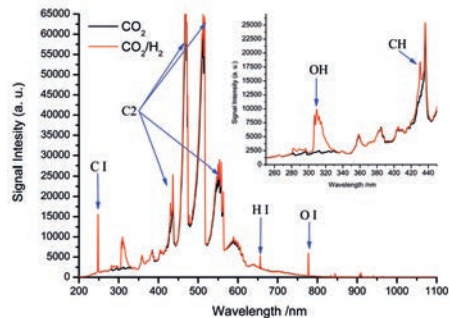


Fig. 2: Image of the emissions spectrum in the range of 200 nm to 1100 nm. The spectrum shows the CO₂ plasma (black) and the CO₂/H₂ plasma (red).

Funding: German Federal Ministry of Education and Research (BMBF), “NEXT GENERATION PLASMA CONVERSION: Integration von “grünem Wasserstoff” in die Plasma-Konversion von CO₂”, FKZ: 03SF0618

NO_x production in an atmospheric plasma torch

Mariagrazia Troia, Andreas Schulz, Matthias Walker



Fig. 1: Plasma torch fed by pressured air with four tangential inlets, here without the sampling apparatus for NO_x detection.

In the current political and global scenario, flexible, sustainable and green avenues for the production of basic chemicals necessary for large-scale industry, able to successfully supplant more traditional methods, are becoming a major focus of interest. In one of such possibilities, the Haber-Bosch method for the production of ammonia, at least one of the intermediate, traditional steps may be substituted by a plasma-assisted synthesis. By means of an atmospheric-pressure, microwave-sus-

tained plasma torch, the mechanisms for the synthesis of nitrogen-based oxides starting from air have been thus investigated.

Concentrations of the thus produced NO, NO₂ and N₂O₄ species, expressed as percentages after a calibration step with the relative reference gases, have been determined by real-time Fourier-Transform Infrared (FTIR) absorption spectroscopy. Results thus far, shown for the standard configuration of the plasma torch, are shown as a function of feed gas flow and operating powers in Fig. 2, and show good accordance with the first investigations carried out by our group in the past.

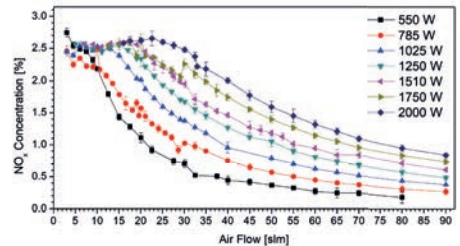


Fig. 2: Total concentration of NO_x species produced as a function of the air flow feeding the plasma torch for different operating powers.



Cross-linking and permeability of polyvinyl alcohol coatings for the humidification of fuel cells

Andre Michele, Alexander Southan, Günter Tovar

Regarding to emissions and imminent bans on cars with combustion engines, the poly electrolyte membrane fuel cell (PEMFC) is a promising technology for automotive applications. The performance is dependent on the state of electrolyte membrane (EM) hydration. Returning excess water generated at the fuel cell's cathode to the EM, is the most sustainable way for optimal water management. This could be carried out by using a humidifier membrane. The selectivity towards reaction gases of this membrane may be improved by using a hydrogel coating.

Polyvinyl alcohol (PVA) is a hydrophilic polymer with interesting properties for the formation of sustainable hydrogel coatings, e. g. good film forming. Moreover, its good water solubility allows ecologic processing without organic

solvents. On the other hand, its solubility makes cross-linking necessary to prevent strong swelling and dissolution of the polymer in water.

Therefore, PVA is cross-linked with the cross-linking agent toluenesulfonic acid (TSA) or modified with benzophenone (BP) moieties to enable UV-light induced self cross-linking. Membranes are formed by dip-coating or doctor blading of porous substrates. The hydrogel formation occurs after activation with heat or UV radiation. In order to avoid performance loss, the stability, water vapor permeation and selectivity against nitrogen are tested at working conditions of the fuel cell.

The thermal cross-linking of PVA in the presence of TSA was investigated via a design of experiments approach.

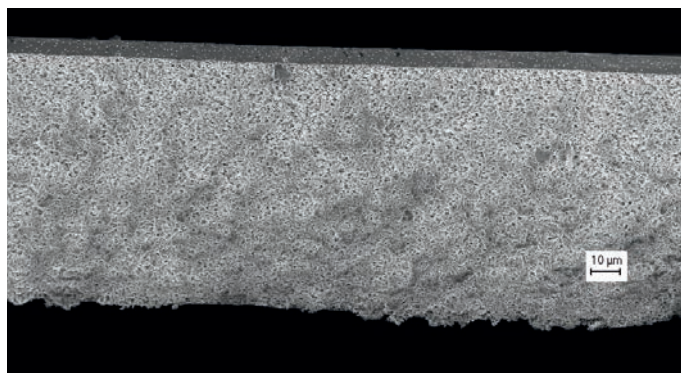


Fig. 1: SEM image of a cross-linked hydrogel film on a porous membrane carrier foil.

With the results, statistical models of the cross-linking process were obtained. For all applied parameters, the formation of an insoluble material and black coloration were observed. These observations could be explained by the parallel cross-linking of PVA and decomposition by dehydration and oxidation. However, the evaluation of the established models allowed the identification of optimal crosslinking parameters with minimal decomposition.

The development of synthesis protocols for benzophenone modified PVA (PVA-BP) was successful. By irradiating PVA-BP films with UV light, they were cross-linked and covalently bound to the substrate. A model based on percolation theory was applied to study the crosslinking reaction. A correlation between the degree of benzophenone modification and the rate of cross-linking was thereby established. The equilibrium swelling degree (EDS) decreased as the irradiation progressed. This could be explained by the decrease in the mesh size of the network.

The investigated membranes with PVA-based coatings were impermeable for nitrogen, but well permeable for water vapor. Consequently, it can be concluded, that the membranes are suitable for the humidification of automotive fuel cells and can therefore provide a decent contribution to sustainable transport of goods and people.

Publications: Michele, A., Paschkowski, P., Hanel, C., Tovar, G. E. M., Schiestel, T., Southan, A.* (2022) Acid catalyzed cross-linking of polyvinyl alcohol for humidifier membranes, *Journal of Applied Polymer Science*, 139, 16. <https://doi.org/10.1002/app.51606>
Michele, A., Luft, D., Tovar, G. E. M.*, Southan, A.* (2022) Photo-crosslinking and surface-attachment of PVA nanocoatings by C,H insertion to customize their swelling behavior and stability in polar media, *Polymer Chemistry*, 10.1039/D2PY00443G. <https://doi.org/10.1039/D2PY00443G>

Collaboration: Fraunhofer Institute for Interfacial Engineering and Biotechnology IGB, Stuttgart; Mahle Filtersysteme GmbH, Stuttgart; Fumatech BWT GmbH, Bietigheim-Bissingen; University of Regensburg, Institute of organic chemistry, Regensburg

Funding: German Federal Ministry for Economic Affairs and Energy (BMWi), promotional reference 03ET6091D



Organic waste as a renewable resource – conversion of the fat and protein content of *Hermetia illucens*

Christian Schmidle, Susanne Zibek, Günter Tovar

Hermetia illucens (Black Soldier Fly, BSF) could be the solution to the growing organic waste problem. In 2016 alone about 1/3 of the food produced, almost 1.3 billion tones, was wasted. [1] With the help of BSF larvae, waste can be converted into fat, protein and chitin. These in turn can be synthesized into higher value products. Because of the similarity of the fatty acid spectrum of the BSFL to tropical fats like coconut or palm kernel oil, the obtained fat could be used to substitute them.

The fat of the BSFL can be transesterified to the methyl esters (FAME). For the conversion, the triglycerides are first transesterified to fatty acid methyl ester. Because of the high degree of free fatty acids present in the BSFL oil, this has to happen in two steps. First an acid catalyzed transesterification with methanol to esterify the free fatty acids, then a basic esterification with NaOH and MeOH to completely convert the triglycerides to the corresponding esters.



Fig. 1: Press cake, filtered fat and dried BSFL
©Fraunhofer IGB



Fig. 2: Extracted BSFL fat
©Fraunhofer IGB

In order to obtain higher quality products such as lubricants or hydraulic oils, a further transesterification is required, in which the methyl group is replaced by di- or triols with different structures in order to achieve a different physico-chemical behavior.

Biosurfactants like APGs require a different pathway. For these surfactants, the fatty acid must be catalytically hydrogenated to the fatty alcohol. This can then be converted to the corresponding APG, e.g. with glucose in the Fischer glycosidation process.

Publication: [1] Surendra, K. C., Olivier, R., Tomberlin, J. K., Jha, R., Khanal, S. K. (2016) Renewable Energy, 98, 197–202. <https://doi.org/10.1016/j.renene.2016.03.022>

Collaboration: Fraunhofer Institute for Interfacial Engineering and Biotechnology, Stuttgart (Koordination); Biopro Baden-Württemberg GmbH, Stuttgart; *Hermetia Baruth GmbH*, Baruth/Mark Brandenburg; ifeu – Institute for Energy and Environmental Research Heidelberg GmbH; University of Stuttgart, Institute for Sanitary Engineering, Water Quality and Solid Waste Management (ISWA); PreZero Foundation & Co. KG, Neckarsulm (associated partner)

Funding: Baden-Württemberg Ministry of the Environment, Climate Protection and the Energy Sector and the European Union funding the project “InBiRa” as part of the ERDF (European Research and Development Fund) program “Bioeconomy – Biorefineries for the recovery of raw materials from waste and wastewater”

11 SUSTAINABLE CITIES AND COMMUNITIES



Immobilization of microalgae in hydrogels

Tugce Demiral, Linus Stegbauer, Günter Tovar



In today's modern world cities occupy 2% of the earth's surface and they consume 75% of the total energy. Urban structures absorb and retain solar irradiation during the day and then slowly dissipate at night. As a result, the city's temperature increases relative to the surrounding rural area, which is a phenomenon called the urban heat island (UHI) effect.

With global warming, it is known that more energy is consumed for cooling the infrastructures rather than to heat them. Therefore to reduce the UHI effect, many strategies are followed and one of the new promising areas is photosynthetic species-embedded living materials. Current systems have the major drawback of requiring completely new construction, subsequently hindering the realization of further buildings for the already existing cities.

Our research project focuses on the design and fabrication of hybrid hydrogels with immobilized microalgae for facades system that can be implemented in any extant building. We aim to have a completely sustainable biological system that serves as a cooling agent for more futuristic living urban structures.

In the present research the biocompatibility and stability of different green microalgae strains are tested with various hydrogel materials to form microalgae-embedded thin-layer gels.

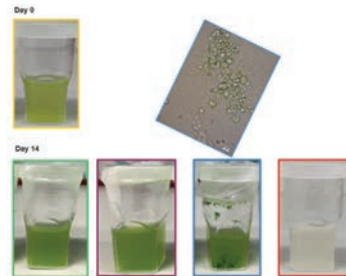
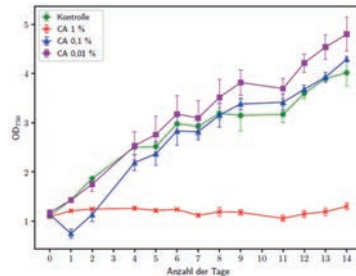


Fig. 1: The biocompatibility of *C. Vulgaris* in different percentages of Chitosan acetate (CA) is determined via optical density measurements at 750 nm (OD_{750}) over 14 days in CellDeg photobioreactors. Pictures of the samples are taken every day as well as light microscopy images for morphological analysis. On day zero, all the samples including the control (only microalgae) have the same OD_{750} , here exemplarily seen in a photobioreactor which is highlighted with a yellow frame. Pictures of the CellDeps on day 14 are shown on the right color-coded according to the lines of the OD_{750} in the left plot.

Collaboration: Fraunhofer Institute for Interfacial Engineering and Biotechnology IGB, Stuttgart

Funding: Elite-Postdoc of Linus Stegbauer, Baden-Württemberg Stiftung

Application of adhesion-promoting layers via plasma polymerisation on glass fibers

Mariagrazia Troia, Andreas Schulz, Matthias Walker

Fiberglass consists of a plastic matrix in which glass fibers are embedded, in order to improve its mechanical properties such as strength and elasticity. The aim of the current project is to improve the adhesion at the fibers-matrix interface and produce light and robust materials for the automotive and aircraft industry. To do so, the fibers have to be coated with a thin film with the required chemical composition and functional groups. The process is carried out by means of an atmospheric plasma torch in which gaseous precursors polymerize and form an ultra-thin film directly on the fibers' surface. The monitoring of the deposition process includes, but it is not limited to, optical emission spectrometry, mostly in the ultraviolet range, in order to determine the spatially-resolved active species concentrations in the plasma, as observed in Fig. 1. A virtual model of the deposition chamber and its plasma torches, as shown in Fig. 2, has moreover been created in order to carry out cold gas simulations, thus providing insight of the process diagnostic and its further optimization.

Collaboration: Plasma Air AG, Weil der Stadt-Hausen; Plasmatrete GmbH, Steinhagen; Institute of Textile Technology (ITA) of RWTH Aachen University, Aachen

Funding: German Federal Ministry for Economic Affairs and Energy (BMWi), project No. ZF44146042P9

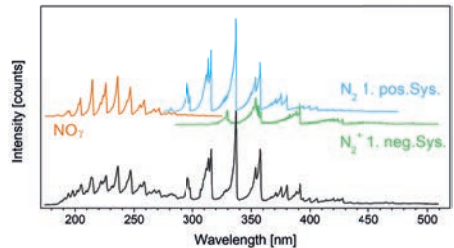


Fig. 1: Optical emission spectroscopy in the ultraviolet range of the air plasma (black) with the isolated contributions of the three main band systems (orange, blue and green).

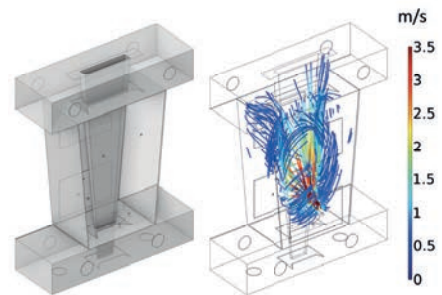


Fig. 2: Model of the reactor's prototype (left) and cold gas simulation's results in case of a single atmospheric torch attached to the deposition chamber. The scale refers to the gas outgoing velocities.

12 RESPONSIBLE
CONSUMPTION
AND PRODUCTION



Synthesis and investigation of hybrid structural composites

Nina Oehlsen, Linus Stegbauer,
Günter Tovar



It is well known that so-called nano-composites have often superior mechanical properties regarding elasticity and hardness. Nano-composites are materials made out of a matrix embedded with particles, which sizes are in the nanometer range. The most common example of a man-made nano-composite is the use of silica or carbon black in tires. In nature the strengthening effect of nano-particles can be found e.g. in teeth of invertebrates.

The aim of this project is to produce and understand nanocomposites which consists of biopolymers and minerals. The inspiration for this is found in nature. Thus, one part of the project is to investigate the stylet of Nemertean species *Amphiporus Lactifloreus*. The other part of the project, the synthesis of nanocomposites, e.g. a gelatin-amorphous calcium phosphate composite showed promising results in terms of mechanical properties and will be studied further. Moreover, nanocomposites with different particle and matrix materials will be investigated with the goal to replace non-recyclable materials like plastics in different areas in the future.

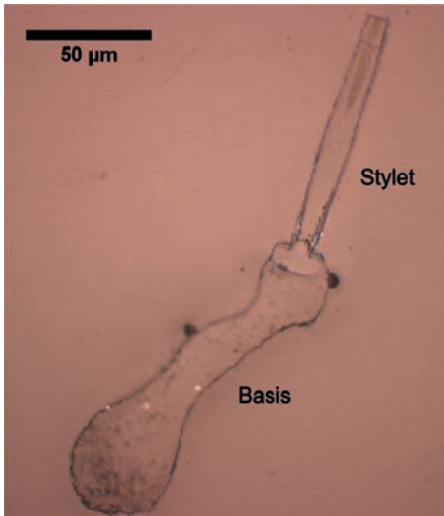


Fig. 1: Microscope image of central stylet with basis of Nemertean species *Amphiporus Lactifloreus* after embedding in epoxy and polishing.

Collaboration: Fraunhofer Institute for Interfacial Engineering and Biotechnology IGB, Stuttgart; S. Weiner, Weizmann Institute of Science, Rehovot, Israel; J. von Döhren, Institut für Evolutionsbiologie und Ökologie, Bonn

Funding: Chitin Fluid (supported by the Carl Zeiss Foundation); PhD scholarship of Verband der Chemischen Industrie e. V. (VCI)

Tribology system for cold sheet metal forming based on volatile lubricants

Paul Reichle, Günter Tovar



Regarding the reduction of material loss during the production process, sheet metal forming is one of the most effective technologies in manufacturing. However, usually mineral oil based lubricants are utilized to decrease friction and wear within the forming process. In addition, these lubricants often contain additives which are toxic to humans and the environment. Typically, the oil is applied on the sheets before the forming process and then removed afterwards in preparation for further process steps like coating. Thus, a decrease of the usage of classical lubricants not just only reduces costs and process time, but the environmental impacts can be lowered, too. One approach is to use volatile lubricants such as nitrogen (N_2) or carbon dioxide (CO_2) for lubrication. Therefore, the media is injected during the forming process into the interstice between sheet and forming tool through laser drilled microinjectors with a diameter of around $350\ \mu m$ (comparable to a steam iron). The injection pressure of the volatile media ranges from 60 bar with CO_2 up to 150 bar by using N_2 . For a better understanding of the friction and wear behaviour of dry metal contacts in the presence of a volatile lubricant, a novel high pressure tribometer was designed. Thus it is now possible to emulate the tribological conditions during forming processes with different volatile lubricants.



Fig. 1: Novel high pressure tribometer to investigate friction and wear of dry metal contacts in volatile lubricant environments.

Publications: Reichardt, G., Henn, M., [...], Tovar, G. E. M. (2022) Friction and Wear Behavior of Deep Drawing Tools Using Volatile Lubricants Injected Through Laser-Drilled Micro-Holes, *The Journal of The Minerals, Metals & Materials Society (JOM)*, 74, 826–836. <https://doi.org/10.1007/s11837-021-05028-8>
 Reichardt, G., Henn, M., [...], Tovar, G. E. M. (2021) Investigations on the Process Stability of Dry Deep Drawing with Volatile Lubricants Injected Through Laser-Drilled Microholes, *TMS 2021 150th Annual Meeting & Exhibition Supplemental Proceedings, The Minerals, Metals & Materials Series*, 230–246. https://doi.org/10.1007/978-3-030-65261-6_21
 Reichardt, G., Henn, M., [...], Hirth, T. (2020) Tribological system for cold sheet metal forming based on volatile lubricants and laser structured surfaces, *Dry Met, Forming OAJ FPR*, 6, 128–165. <http://dx.doi.org/10.26092/elib/156>

Collaboration: Barz, J. and Umlauf, G., Fraunhofer Institute for Interfacial Engineering and Biotechnology IGB, Stuttgart; Henn, M., Holder, D. and Graf, T., Institut für Strahlwerkzeuge IFSW, University of Stuttgart; Reichardt, G. and Liewald, M., Institute for Metal Forming Technology IFU, University of Stuttgart

Funding: German Research Foundation (DFG), SPP 1676: Dry Metal Forming – Sustainable Production through Dry Processing in Metal Forming (TO211/3-2), for further information visit www.trockenumformen.de



Design of a nozzle geometry for the formation of an atmospheric pressure microwave plasma flow

Andreas Schulz, Katharina Wieggers, Matthias Walker

After the generation of a plasma for the plasma-chemical synthesis, the management of the reactions in the outflowing plasma is of the greatest importance. The desired radicals are formed in the hot atmospheric pressure plasma, which, however in the afterglow zone, either react back to the original starting compounds or to side-products. To prevent this, the effluent plasma must be cooled down as quickly as possible. With the help of a suitable nozzle shape and a suitable flow guide, the plasma can be forced to follow the given geometry. Due to the forced increase in cross-section, the effluent cools down and quenches the current chemical composition. The

cross-section of the nozzle geometry is shown schematically in Fig. 1. Fig. 2 shows the plasma that is just flowing straight out. By adapting the gas flow, the plasma is forced into the nozzle shape and cooled down considerably, as can be seen in Fig. 3.

Collaboration: Max Planck Institute for Plasma Physics (IPP), Garching; Karlsruhe Institute of Technology (KIT), Karlsruhe; Forschungszentrum Jülich (FZ-Jülich), Jülich; University of Augsburg, Augsburg

Funding: Cooperation agreement between the Max Planck Institute for Plasma Physics (IPP) and the University of Stuttgart in the field of plasma gas conversion "Plasma4Gas" in the "Materials and Technologies for the Energy Transition" program of the research field Energy of the Helmholtz Association of German Research Centers e.V.

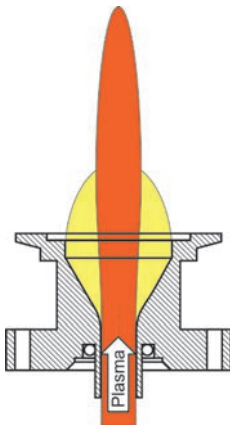


Fig. 1: Scheme of the nozzle design with the two modes.

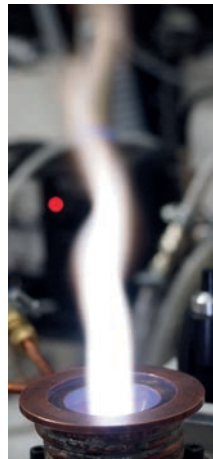


Fig. 2: Image of the strait effluent plasma.

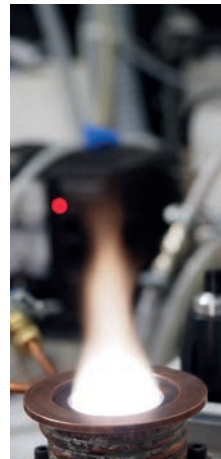


Fig. 3: Image of the extended effluent plasma.

13 CLIMATE
ACTION



Numerical investigation of a microwave plasma torch for CO₂ decomposition

Stefan Merli, Andreas Schulz, Matthias Walker, Katharina Wieggers, Marc Bresser

The atmospheric microwave plasma torches, which are currently developed and investigated at IGVP for CO₂ decomposition (see contributions from A. Schulz, K. Wieggers), are also being studied numerically in Comsol Multiphysics to increase the efficiency of the process. Since gas flow plays an important role in the reactor, CFD simulations were performed, considering the hot plasma zone only as a heat source. With this, a lot of information can be gained about important parameters like flow velocity, gas pressure, temperature distribution as well as about zones where laminar, turbulent, rotational or backward flows occur. The advantage of such simulations is that many different geometrical variations, like nozzle shapes and sizes, can be investigated without actually manufacturing it.

The simulations have shown that the nozzle and the subsequent expansion zone play an important role, on the one hand for mixing of the hot gas from the plasma zone and the cold gas from the enveloping rotational flow and on the other hand for quenching reverse reactions through cooling after the nozzle. Fig. 1 shows an example for a reverse vortex configuration with a hollow temperature profile in the expansion zone.

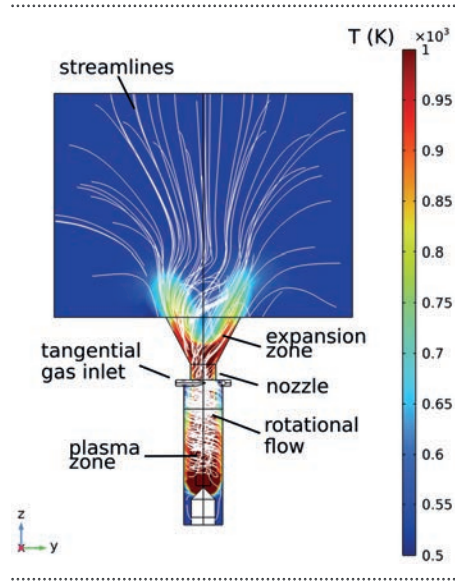


Fig. 1: Streamlines and gas temperature distribution for a reverse vortex configuration.

In the next step, temperature dependent chemical reactions for the CO₂ decomposition will be added to optimize the geometry for a higher efficiency.

Collaboration: Max Planck Institute for Plasma Physics (IPP), Garching; Karlsruhe Institute of Technology (KIT), Karlsruhe; Forschungszentrum Jülich (FZ-Jülich), Jülich; University of Augsburg, Augsburg

Funding: Cooperation agreement between the Max Planck Institute for Plasma Physics (IPP) and the University of Stuttgart in the field of plasma gas conversion "Plasma4-Gas" in the "Materials and Technologies for the Energy Transition" program of the research field Energy of the Helmholtz Association of German Research Centers e.V.

Enhancing CO₂ conversion through an optimization in the gas management

Katharina Wieggers, Andreas Schulz, Matthias Walker, Günter Tovar

Currently, the basic chemical CO is produced by and from fossil fuels. But because of the climate crisis, various alternative methods are being studied intensively. A well-known process is the electrochemical reduction of CO₂. Another method is the dissociation of CO₂ in a plasma process. However, to become competitive with electrolysis, the CO₂ conversion to CO in the plasma must be increased. Therefore, the back reaction to CO₂ has to be suppressed to improve the plasma process. For this purpose, the gas management is enhanced by a nozzle. Fig. 1 shows the geometry of the nozzle, in which the hot plasma core and the cold gas envelope are forced to pass together through the restriction with a diameter of 10 and 5 mm, respectively. As oxygen is produced and oxygen separation has to be improved, the gas is expanded in a nozzle, to be ripped open after the restriction. This way, as much plasma area as possible is available for the surface-sensitive separation process. Fig. 2 shows the effect on the conversion measurements. The nozzle with a diameter of 10 and 5 mm increase the conversion significantly by a factor of 2 and 4, respectively.

Funding: Federal Ministry of Education and Research (BMBF) as part of the Kopernikus Project PiCK "Plasma induzierte CO₂-Konversion" (Funding Code: 03SFK2S3A).

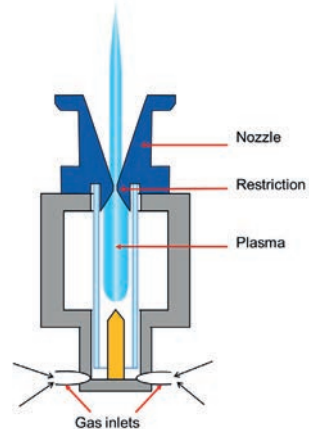


Fig. 1: Geometric sketch of the nozzle.

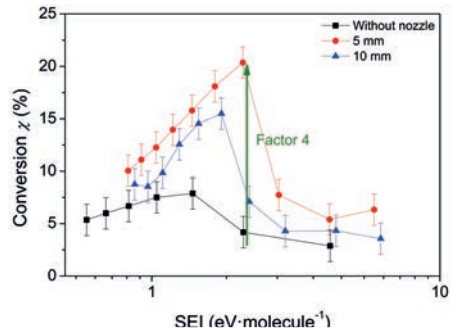


Fig. 2: Comparison of the conversion measurements for the standard setup (black) and the nozzle configuration. The restriction of the nozzle is 5 mm (red) and 10 mm (blue), respectively. The conversion can be increased by a factor of 4 for using a nozzle with a 5 mm restriction.

Oxygen separation with ceramic hollow fibers in a CO₂ plasma

Katharina Wieggers, Andreas Schulz, Matthias Walker, Günter Tovar

The goal of the Paris Agreement from 1995 is to limit global warming to less than 2°C, preferably to 1.5°C. To achieve this long-term temperature goal, a significant avenue is the electrification of the chemical industry. Besides the well-known electrolysis processes, plasma processes are gaining more and more interest. An auspicious process is the plasma conversion of CO₂ in CO and O₂. In order to provide the purest possible CO gas for the chemical industry, the O₂ must be removed from the gas mixture. For this purpose, ceramic hollow fibers consisting of La_{0.6}Ca_{0.4}Fe_{0.2}Co_{0.8}O_{3-d} (LCCF) are used. Fig. 1 shows the LCCF fiber in the plasma-membrane reactor. At 750°C and above, oxygen starts to permeate into the fiber. The LCCF fibers are temperature stable up to about 1200°C.

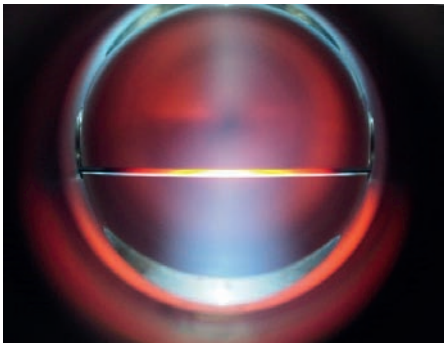


Fig. 1: LCCF fiber inside the plasma-membrane-reactor at CO₂ flow of 6 slm CO₂ and a MW power of 0.77 kW

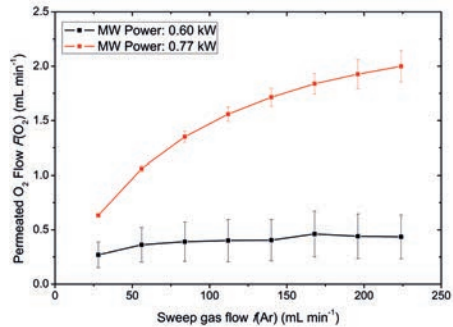


Fig. 2: Oxygen permeation of a LCCF fiber at different sweep gas flows.

The driving force of oxygen permeation is the oxygen partial pressure gradient. The oxygen permeation depends on the temperature (diffusion), the surface exchange coefficient (material) and the sweep gas flow inside the fiber (oxygen partial pressure gradient). Fig. 2 shows the permeated oxygen flow $F(\text{O}_2)$ against the sweep gas flow $f(\text{Ar})$. The dependence of the sweep gas flow is only noticeable at a microwave (MW) power of 0.77 kW because more oxygen is permeating through the fiber. To maintain an oxygen partial pressure gradient, the permeated oxygen has to be removed by a higher $f(\text{Ar})$. Additionally, $F(\text{O}_2)$ increases with raising MW power at a constant CO₂ flow of 6 slm because the temperature inside the plasma membrane reactor increases.

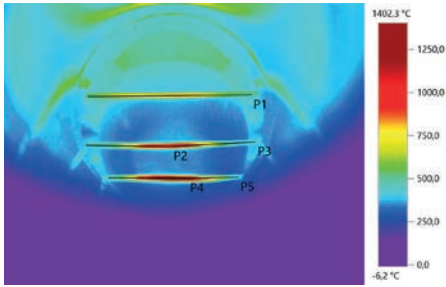


Fig. 3: The picture is taken with the thermal camera with an emission coefficient of $\epsilon = 0.48$. Three fibers are arranged above each other. The lowest fiber is the nearest to the plasma zone and exhibits the highest temperature.

Because the next step is to increase the number of fibers inside the reactor to separate more O_2 from the plasma gas, three fibers are aligned vertically above each other. Each fiber's temperature profile can be fitted with a Gaussian profile, as shown in Fig.4. The closer a fiber is to the plasma zone, the higher its temperature.

Collaboration: Frederic Buck, Fraunhofer Institute for Interfacial Engineering and Biotechnology IGB, Stuttgart; Thomas Schiestel, Fraunhofer Institute for Interfacial Engineering and Biotechnology IGB, Stuttgart

For this reason, the temperature is monitored with a thermal camera (TC), while a thermoelement (TE) is used to determine the emission coefficient and validate the TC values. Fig.3 shows the picture of the TC with an emission coefficient of $\epsilon = 0.48$ for around 1200 °C.

Funding: Federal Ministry of Education and Research (BMBF) as part of the Kopernikus Project PiCK "Plasma induzierte CO_2 -Konversion" (Funding Code: 03SFK2S3A).

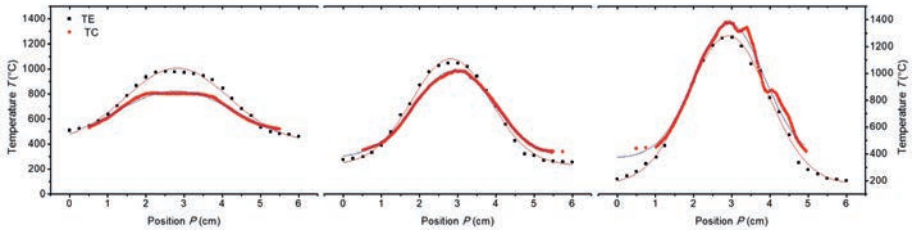


Fig. 4: Temperature profile of the fibers. The values are determined via a thermal imaging camera and a thermoelement measurements. The temperature is dependent on the position of the fiber. The operation parameters are 6 slm CO_2 and a MW power of 0.77 kW.



High-temperature oxygen separation performance of dual-phase ceramic material

Katharina Wieggers, Andreas Schulz, Matthias Walker, Günter Tovar

Climate change is accelerating, making it even more important to electrify the chemical industry. CO is an essential basic chemical that can be converted into higher-value hydrocarbons. In a plasma torch, CO₂ is decomposed into CO and O₂. An oxygen separation step is included because only CO is the desired product. This should be achieved with oxygen-conducting ceramic hollow fibers. To increase the range of oxygen separation, the temperature-stable dual-phase material (60 wt% Ce_{0.6}Gd_{0.2}O_{1.9} – 40 wt% Gd_{0.85}Ce_{0.15}Fe_{0.75}Co_{0.25}O₃ (GCFCO)) investigated in the research topic “Ceramic membrane material screening for high-temperature oxygen permeation” is tested for its oxygen conductivity. Three fibers are placed at different positions in the plasma membrane reactor: at the middle position (MP), 1.5 cm below the MP (closer to the hot plasma zone), and 1.5 cm above the MP (farther away from the hot plasma zone). Fig. 1 shows the permeated oxygen flux ($F(O_2)$) vs. microwave (MW) power at constant CO₂ flux. The temperature profile is similar to a flame, and since the higher MW power results in higher temperatures in the plasma membrane reactor, $F(O_2)$ increases

with increasing MW power because the oxygen permeation is strongly temperature dependent. Furthermore, the permeation is dependent on the position of the fiber. So, the fiber at the lowest place is exposed to the highest temperatures and shows the highest $F(O_2)$.

Collaboration: Stefan Baumann, Forschungszentrum Jülich, Institute of Energy and Climate Research IEK-1 (Materials Synthesis and Processing), Jülich; Frederic Buck and Thomas Schiestel, Fraunhofer Institute for Interfacial Engineering and Biotechnology IGB, Stuttgart

Funding: Cooperation agreement between the Max Planck Institute for Plasma Physics (IPP) and the University of Stuttgart in the field of plasma gas conversion “Plasma4-Gas” in the “Materials and Technologies for the Energy Transition” program of the research field Energy of the Helmholtz Association of German Research Centers e. V.

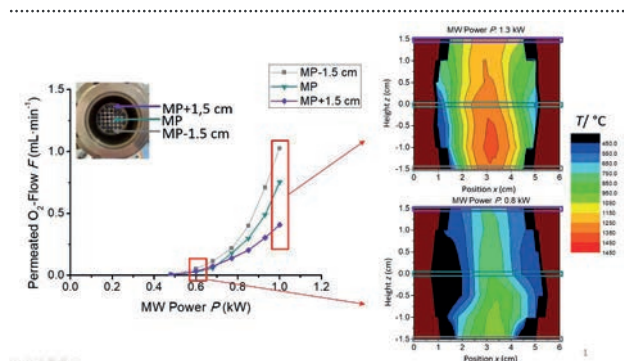


Fig. 1: Vertically resolved oxygen Permeation for GCFCO.

Ceramic membrane material screening for high-temperature oxygen permeation

Katharina Wieggers, Andreas Schulz, Matthias Walker, Günter Tovar

The temperature stability of the LCCF fibers is limited to about 1200 °C. In order to increase the region for O₂ separation in the plasma torch, new ceramic materials with higher temperature resistance have to be developed and investigated. The idea behind this is that, depending on the plasma temperature (i.e. mainly the height in the plasma membrane reactor) different fiber materials can be used.

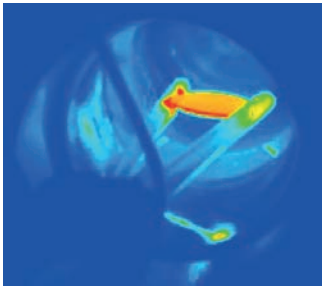


Fig. 1: Sintered pellet in a CO₂ plasma at 6 slm CO₂ and a MW power of 0.93 kW.

These ceramic materials are the so-called MIEC (mixed ionic and electronic conductivity) materials. The first and well-investigated material is La_{0.58}Sr_{0.4}Co_{0.2}Fe_{0.8}O_{3-δ} by Tereoka, and it is used as reference material [1]. The A site cations are changed or a dual-phase material is used to increase the temperature and chemical stability.

Fig. 1 shows a sintered pellet in the plasma. The operating parameters are 6 slm

Material	0.93 kW	1.08 kW
La _{0.58} Sr _{0.4} Co _{0.2} Fe _{0.8} O _{3-δ}	😊	😞
SrTi _{0.75} Fe _{0.25} O _{3-δ}	😊	😞
60 Gew. % Ce _{0.8} Gd _{0.2} O _{1.9} - 40 Gew. % FeCo ₂ O ₄	😊	😊
85 Gew. % Ce _{0.8} Sm _{0.2} O _{1.9} - 15 Gew. % FeCo ₂ O ₄	😊	😊
60 Gew. % Ce _{0.8} Gd _{0.2} O _{1.9} - 40 Gew. % Gd _{0.85} Ce _{0.15} Co _{0.75} Fe _{0.25} O _{3-δ}	😊	😊*

Fig. 2: Table with tested materials. All materials are stable at a MW power of 0.93 kW. However, at a MW power of 1.08 kW the perovskite materials fail. The asterisk means that the pellet has cracked during cooling but does not show any chemical decomposition.

CO₂ with a microwave (MW) power of 1.2 and 1.4 kW. Materials are tested for 15 minutes. Fig. 2 shows in a table the results. The perovskite materials and one of the dual-phase materials fails at a microwave (MW) power of 1.0 kW. However, the other dual-phase materials are also stable at higher powers and higher temperatures.

Publication: [1] Teraoka, Y., Zhang, H.-M., Furukawa, S., Yamazoe, N. (1985) Oxygen permeation through perovskite-type oxides. *Chemistry Letters*, 14 (11), 1743-1746. <https://doi.org/10.1246/cl.1985.1743>

Collaboration: Stefan Baumann, Forschungszentrum Jülich, Institute of Energy and Climate Research IEK-1 (Materials Synthesis and Processing), Jülich; Ursel Fantz, Max Planck Institute for Plasma Physics IPP, Munich

Funding: Cooperation agreement between the Max Planck Institute for Plasma Physics (IPP) and the University of Stuttgart in the field of plasma gas conversion "Plasma4-Gas" in the "Materials and Technologies for the Energy Transition" program of the research field Energy of the Helmholtz Association of German Research Centers e.V.

CO₂ conversion and energy efficiency of a microwave plasma torch

Katharina Wieggers, Andreas Schulz, Matthias Walker, Günter Tovar

Mankind nowadays is strongly affected by ongoing climate change, mainly caused by the increasing emission of carbon dioxide (CO₂). CO₂ is a very stable molecule, but it can however be activated by a plasma process, which converts CO₂ into the value-added chemical molecule CO. The oxygen radicals also produced in the plasma process recombine into molecular oxygen. An important parameter in such a process is the conversion and energy efficiency. Therefore, the volumes of CO₂, CO and O₂ were investigated via two independent analysis methods: Fourier-transformed infrared-spectroscopy (FT-IR) and mass spectrometry (MS). Fig. 1 shows the conversion along the plasma torch. The first measurement point is 14 cm above the ignition tip, because ceramic fibers for the oxygen separation process are placed at this position (see one of the next research topics). The conversion drastically decreases until 29 cm. Then the conversion is stable. From this measuring point onward, the gas is cooled by a chiller, thus thermalized and mixed. Fig. 2 shows the energy efficiency of the thermalized gas: 25% of the used energy is stored in CO for the operating parameter 12 slm CO₂ and 0.48 kW microwave power.

Funding: Federal Ministry of Education and Research (BMBF) as part of the Kopernikus Project PiCK "Plasma induzierte CO₂-Konversion" (Funding Code: 03SFK2S3A)

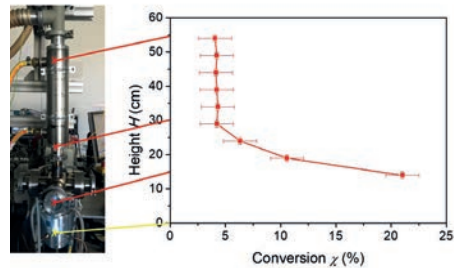


Fig. 1: The height profile of the conversion along the exhaust gas tube. At the height of 29 cm the conversion values become stable. The measurement is performed at a CO₂ flow of 9 slm and a microwave power of 1.4 kW.

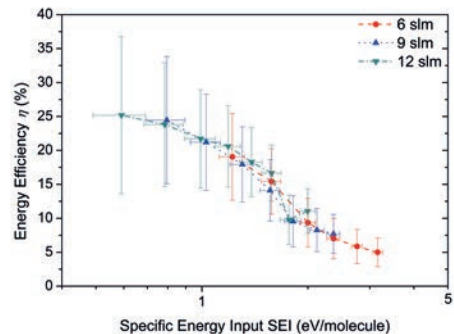


Fig. 2: The energy efficiency of the thermalized gas is plotted against the specific energy input (SEI). In the SEI, the operating parameter of microwave power and CO₂ flow are correlated.

Publication: Wieggers, K., Schulz, A., Walker, M., Tovar, G.E.M., (2022) *Chemie Ingenieur Technik*, 94: 299–308
<https://doi.org/10.1002/cite.202100149>

Photomodulation of the mechanical properties of a chitosan-based composite material

Nils von Seggern, Linus Stegbauer, Günter Tovar

The implementation of stimuli responsive materials in macromolecules is widely recognized as a promising route toward the design of interactive materials. For this context, temperature, mechanical force, magnetic fields or light have been successfully applied. Light often outperforms other stimuli due to its non-invasive character combined with the high energetic and spatiotemporal resolution. Utilizing photoswitches for material preparation is in turn proceeding the fabrication of energy storage systems, actuators, (bio) sensors as well as molecular motors. However, the photomodulation of the mechanical properties of materials continues to pose a challenge. Here, we present light-responsive bulk materials that can reversibly modulate the stiffness and hardness.

By introducing polar head groups in the photoswitch, strong interactions with the chitosan-matrix are enabled. Solid-state UV-Vis spectroscopy and the MAS-solid state NMR revealed a reversible photo-isomerization of the bulk material. Moreover, nanoindentation experiments indicated that the reduced modulus EIT and hardness HM of the responsive material could be modulated by at least 20%, when irradiated with 365 nm. The original mechanical properties could be recovered after keeping the same sample in the dark for 5 days.

Collaboration: Fraunhofer Institute for Interfacial Engineering and Biotechnology IGB, Stuttgart

Funding: Carl Zeiss foundation / Chitinfluid (Grant Agree Number P2019-02-004)

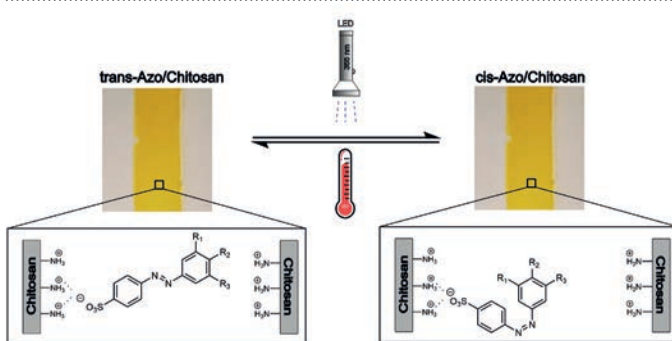


Fig. 1: Schematic representation of the UV-induced isomerization of the photoswitch in the chitosan-matrix.

14 LIFE
BELOW WATER





Optimization of a DBD plasma for the deposition of protective films in heat exchangers

Mariagrazia Troia, Andreas Schulz, Matthias Walker

Protective films in cooling systems of power plants can be beneficial in order to reduce the maintenance costs and improve the former's efficiency and lifetime. The deposition of such coatings directly inside the water pipes can be carried out by means of an atmospheric dielectric barrier discharge (DBD) plasma fed on nitrogen and a precursor for the solid film, with the inner sides of the pipe and a moving steel head acting as electrode pairs.

In order to optimize the process, a model of such reactor has been built and extensive FEM-simulations for the cold gas flow inside the pipe for different geometries of the head have been run. The optimization process includes changes in the geometry of the Teflon ring holding the head in place and the number and position of gas inlets, in order to attain the desired gas velocity and spatial distribution for a homogeneous deposition process, and variations of the geometry of the head's tail, in order to prevent backflows in the plasma afterglow region that could lead to dust formation and its subsequent embedding in the newly-deposited coating. The alternative designs have been based on schemes of existing airships, with the PL25 shown in Fig. 1. providing the best possible outcome over a wide range of gas inlet velocities (up to 30 m/s).

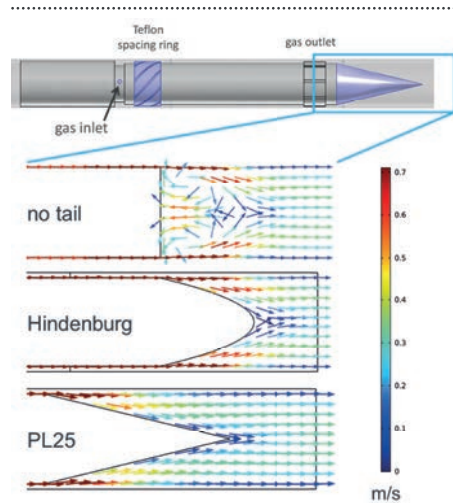


Fig. 1: Above, schematic view of the reactor head inside the pipe, with the optimized components highlighted in blue (gas inlet, teflon ring, tail). Below, gas velocity arrow plots of the tail zone (the blue frame) for the initial head's geometry and two variations based on airships, aimed at minimizing or completely preventing gas backflows in the afterglow region.

Collaboration: Sven Boehler, Siemens AG Corporate Technology, Erlangen; Florian Eder, Siemens AG Corporate Technology, Erlangen

Funding: Industrial project



sPlash – Plasma-coated hydrophobic textiles for cleaning oil spillage in inland waterways

Mariagrazia Troia, Andreas Schulz, Matthias Walker

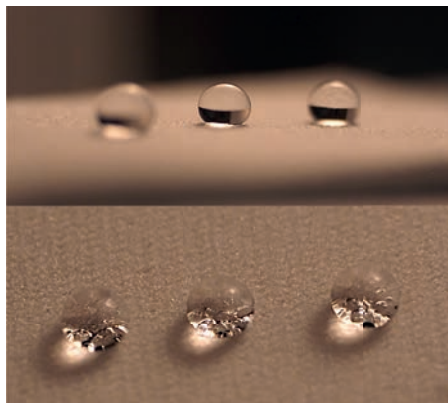


Fig. 1: Above, water droplets sitting on a textile substrate coated with a thin hydrophobic plasma film with an apparent contact angle higher than 150° . A Cassie-Baxter regime is attained, as shown by the small air pockets trapped at the textile-water interface (detail below).

Oil spillages in both open water and inland waterways constitute a serious harm for aquatic life and its environment. Separation of oil from freshwater remains arduous even in case of minor-scale spillages. By adopting a biomimetic approach and taking as example the aquatic fern *Salvinia molesta*, capable of separating water and oil by means of the surface of its leaves, a smart system consisting of a textile substrate coated on both sides with a thin hydrophobic film has been devised. The two films separate oil from water, with the former travelling through the textile fibers by means of capillary forces alone. A basket-like object made of such material should be able, when

immersed in contaminated waters, to separate the oily fraction in a swift, energy-free and repeatable process.

The thin, organosilicon-based hydrophobic films have been produced by means of a low-pressure microwave Electron Cyclotron Resonance (ECR) plasma, fed with mixtures of hydrogen and organosilicon monomers. First tests on coated textile samples show no damages after the process and a complete coverage of the substrates. Apparent contact angles of more than 160° show the presence of a Cassie-Baxter wettability regime, with the samples' properties remaining stable also after under-water aging tests.

Collaboration: Institute of Textile Technology of RWTH Aachen University, Aachen

15 LIFE
ON LAND





Production of the beta-glucan chrysolaminarin from microalgae in closed photobioreactor systems

Konstantin Frick, Susanne Zibek, Günter Tovar

The activities of the IGVP in the field of microalgae biotechnology focused in recent years on the production of chrysolaminarin, a 1,3-1,6-beta-glucan that is produced by diatoms as primary energy storage. There are different possible applications for chrysolaminarin, like in food or feed. In particular, vascular plants react to contact with chrysolaminarin by activating their defence systems against pathogenic fungi. It has been described in the literature that treatment with beta-glucans like chrysolaminarin, can provide some protection against subsequent fungal infection (e.g. *Plasmopara viticola*). Currently, this effect is being tested on grapevines together with project partners in order to reduce the application of fungicides like copper. At IGVP processes for the production of chrysolaminarin in closed photobioreactors were developed. In addition to different microalgae species, the influence of cultivation conditions was investigated. Concerning the chosen cultivation conditions, it was found that especially the amount of light and the nutrient management have a great influence for the productivity and the final chrysolaminarin content. Based on the results, two cultivation scenarios were developed, which are currently being investigated further. Besides cultivation, the extraction of chrysolaminarin from the microalgal biomass was investigated.

In the future, scale-up of the processes will be focused in order to enable further experiments on different applications.

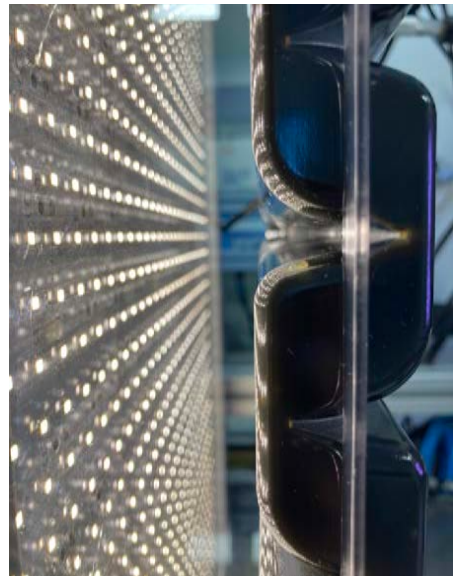


Fig. 1: A culture of the diatom *Phaeodactylum tricorneratum* in an artificially illuminated photobioreactor.

Collaboration: Fraunhofer Institute for Interfacial Engineering and Biotechnology IGB, Stuttgart; University of Hohenheim, Stuttgart; Staatliche Lehr- und Versuchsanstalt für Wein- und Obstbau (LVVO), Weinsberg

Funding: State Ministry of Baden-Wuerttemberg of Sciences, Research and Arts (Fkz.: 7533-10-5-185A); State Ministry of Baden-Wuerttemberg of Food, Rural Affairs and Consumer Protection (Fkz.: BWFE120131 and 54-8214.07-FP20-128/1)



Integrated process design and optimization of cellobiose lipids fermentation and purification

Amira Oraby, Susanne Zibek, Günter Tovar, Steffen Rupp

Research within the biosurfactants field at the IGVP is focused on glycolipids such as Cellobiose lipids (CL), that are produced by *Ustilaginaceae* and show high potential for application in cosmetics or detergents. In our working group, we established a fermentation process coupled with foam fractionation that enables the production of CL with in situ product recovery.

Based on the results of the life cycle assessment and techno-economic analysis of our fermentation process, we were able to identify process steps with the highest contribution to the ecological and economic impact of CL production. Energy demand for aeration and agitation showed the highest environmental impact, while fermentation duration and product titer highly affect the production price. Based on these and further results, process adaptation strategies were proposed and implemented up to a 42 L scale. For application tests, we provide our project partners with samples in the 100 g scale.

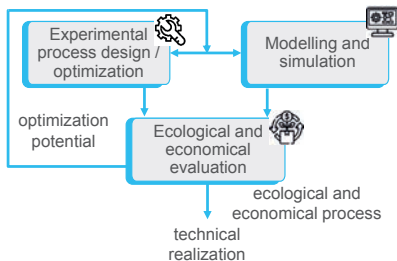


Fig. 1: Schematic illustration of the integrated process design and optimization approach used to identify optimization potential for CL production, based on the results of an ecological and economical evaluation of the process.

In order to pave the way for an industrial application, economic hurdles in terms of high production prices need to be overcome, while increasing the ecological advantage of CL. Therefore, we aimed at identifying economic and ecological process bottlenecks for CL production, and use them as drivers for process optimization.

Publications: Oraby, A., Rupp, S., Zibek, S. (2022) Techno-Economic Analysis as a Driver for Optimisation of Cellobiose Lipid Fermentation and Purification, *Front Bioeng Biotechnol*, 10. <https://doi.org/10.3389/fbioe.2022.913351>
Oraby, A., Weickardt, I., Zibek, S. (2022) Foam fractionation methods in aerobic fermentation processes, *Biotechnol Bioeng*, 119, 1697–1711. <https://doi.org/10.1002/bit.28102>

Collaboration: Fraunhofer Institute for Interfacial Engineering and Biotechnology IGB, Stuttgart

Funding: Deutsch Bundesstiftung Umwelt DBU (German Federal Environmental Foundation), AZ: 80017/333; German Federal Ministry of Education and Research (BMBF), funding code: 031B0469P and 031B1059P



Mineral composites as DBD layers in a plasma-adsorber-scrubber-system for waste air treatment

Mariagrazia Troia, Andreas Schulz, Matthias Walker

In order to decrease air pollution caused by bio-sources, a plasma dielectric barrier discharge (DBD) can be employed in the treatment for the decomposition of pollutant gases such as methane. The plasma is ignited in air via a high voltage applied to the electrode pairs. The ceramic barriers acting as dielectric are embedded with TiO₂ particles, which act as photo-catalysts in the oxidation of CH₄ to CO₂ and H₂O. Such barriers must be able to withstand prolonged exposure to the plasma without breaking down, while at the same time being as light (i.e. less dense) as possible, in order to reduce the weight and the costs of the overall reactor. To this end, the density and the lifetime in plasma of tens of samples with different chemical compositions and manufacturing methods have been evaluated, as reported in Fig. 1 and 2. Densities below a certain threshold cause inevitable breakdowns in the samples, but even in case of much higher average values a residual microporosity may still cause the plates to be unable to withstand the plasma, as shown by sample 17.

Collaboration: Plasma Air AG, Weil der Stadt-Hausen; Institute for Sanitary Engineering, Water Quality and Solid Waste Management (ISWA), Stuttgart; Institute of Textile Technology (ITA) of RWTH Aachen University, Aachen; Richter Akustik & Design GmbH & Co, Melle

Funding: German Federal Ministry for Economic Affairs and Energy (BMWi), project No. ZF4414602CM7

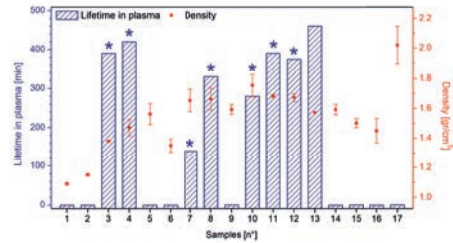


Fig. 1: Density and lifetime in plasma for different samples acting as a dielectric barrier. The asterisks mark the samples never undergoing a breakdown.

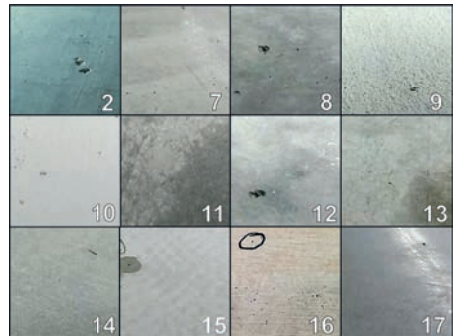


Fig. 2: Surfaces of a selection of the samples tested in the plasma (numbers corresponding to those of Fig. 1). In some cases it is also possible to observe the punch-throughs caused by the barrier breakdown, as for samples 2, 8, 9, 12, 15, 16 and 17.

University of Stuttgart

Nobelstrasse 12
70569 Stuttgart
Germany

Contact

Prof. Dr. habil. Günter Tovar
Phone +49 711 685-62304
Fax +49 711 685-63102
institut@igvp.uni-stuttgart.de

www.igvp.uni-stuttgart.de

